

Positive Cooperativity in the Template-Directed Synthesis of Monodisperse Macromolecules

Matthew E. Belowich,[†] Cory Valente,[†] Ronald A. Smaldone,[†] Douglas C. Friedman,[†] Johannes Thiel,[‡] Leroy Cronin,^{*,‡} and J. Fraser Stoddart^{*,†,§}

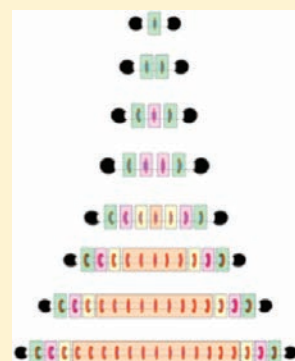
[†]Department of Chemistry, Northwestern University, 2145 Sheridan Road, Evanston, Illinois 60208-3133, United States

[‡]School of Chemistry, University of Glasgow, University Avenue, Glasgow G12 8QQ, United Kingdom

[§]NanoCentury KAIST Institute and Graduate School of EEWS (WCU), Korea Advanced Institute of Science and Technology (KAIST), 373-1 Guseong Dong, Yuseong Gu, Daejeon 305-701, Republic of Korea

Supporting Information

ABSTRACT: Two series of oligorotaxanes **R** and **R'** that contain $-\text{CH}_2\text{NH}_2^+\text{CH}_2-$ recognition sites in their dumbbell components have been synthesized employing template-directed protocols. [24]Crown-8 rings self-assemble by a clipping strategy around each and every recognition site using equimolar amounts of 2,6-pyridinedicarboxaldehyde and tetraethyleneglycol bis-(2-aminophenyl) ether to efficiently provide up to a [20]rotaxane. In the **R** series, the $-\text{NH}_2^+$ recognition sites are separated by trimethylene bridges, whereas in the **R'** series the spacers are *p*-phenylene linkers. The underpinning idea here is that in the former series, the recognition sites are strategically positioned 3.5 Å apart from one another so as to facilitate efficient $[\pi\cdots\pi]$ stacking between the aromatic residues in contiguous rings in the rotaxanes and consequently, a discrete rigid and rod-like conformation is realized; these noncovalent interactions are absent in the latter series rendering them conformationally flexible/nondiscrete. Although in the **R'** series, the [3]-, [4]-, [8]-, and [12]rotaxanes were isolated after reaction times of <5–30 min in yields of 72–85%, in the **R** series, the [3]-, [4]-, [5]-, [8]-, [12]-, [16]-, and [20]rotaxanes were isolated in <5 min to 14 h in 88–98% yields. It follows that while in the **R'** series the higher order oligorotaxanes are formed in lower yields more rapidly, in the **R** series, the higher order oligorotaxanes are formed in higher yields more slowly. In the **R** series, the high percentage yields are sustained throughout, despite the fact that up to 39 components are participating in the template-directed self-assembly process. Simple arithmetic reveals that the conversion efficiency for each imine bond formation peaks at 99.9% in the **R** series and 99.3% in the **R'** series. This maintenance of reaction efficiency in the **R** series can be ascribed to positive cooperativity, that is, when one ring is formed it aids and abets the formation of subsequent rings presumably because of stabilizing extended $[\pi\cdots\pi]$ stacking interactions between the arene units. Experiments have been performed wherein the dumbbell is starved of the macrocyclic components, and up to five times more of the fully saturated rotaxane is formed than is predicted based on a purely statistical outcome, providing a clear indication that positive cooperativity is operative. Moreover, it would appear that as the **R** series is traversed from the [3]- to the [4]- to the [5]rotaxane, the cooperativity becomes increasingly positive. This kind of cooperative behavior is not observed for the analogous oligorotaxanes in the **R'** series. The conventional bevy of analytical techniques (e.g., HR-MS (ESI) and both ¹H and ¹³C NMR spectroscopy) help establish the fact that all the oligorotaxanes are pure and monodisperse. Evidence of efficient $[\pi\cdots\pi]$ stacking between contiguous arene units in the rings in the **R** series is revealed by ¹H NMR spectroscopy. Ion-mobility mass spectrometry performed on the **R** and **R'** series yielded the collisional cross sections (CCSs), confirming the rigidity of the **R** oligorotaxanes and the flexibility of the **R'** ones. The extended $[\pi\cdots\pi]$ stacking interactions are found to be present in the solid-state structures of the [3]- and [4]rotaxanes in the **R** series and also on the basis of molecular mechanics calculations performed on the entire series of oligomers. The collective data presented herein supports our original design in that the extended $[\pi\cdots\pi]$ stacking between contiguous arene units in the rings of the **R** series of oligorotaxanes facilitate an essentially rigid rod-like conformation with evidence that positive cooperativity improves the efficiency of their formation. This situation stands in sharp contrast to the conformationally flexible **R'** series where the oligorotaxanes form with no cooperativity.



INTRODUCTION

Molecules which contain mechanical bonds¹ have been targets of interest to synthetic chemists ever since the first reported synthesis of a catenane by Wasserman² in 1960. Early approaches to the syntheses of rotaxanes as well as catenanes evolved from being all but statistical^{2,3} in the beginning, a strategy which

suffers from yields of less than 1%, to strategies using covalent templates⁴ which generally improved the yields but require many (commonly >20) synthetic steps. In 1983, Sauvage and

Received: December 7, 2011

Published: February 3, 2012

co-workers^{5,6} opened up the field of mechanically interlocked molecules¹ (MIMs) when they introduced metal-templating⁷ as an efficient synthetic route to catenanes and rotaxanes. Their seminal work represented a paradigm shift in the way MIMs were prepared. This important advance led⁸ to the uncovering of noncovalent templates based on solvophobic forces,⁹ donor–acceptor interactions,¹⁰ hydrogen bonding, both neutral¹¹ and charged,¹² electrostatic interactions involving anions,¹³ and, most recently, radicals.¹⁴

Pedersen's serendipitous discovery¹⁵ of the crown ethers¹⁶ and the fact that they form complexes with organic as well as metal cations is widely regarded today as having marked a defining moment which led to the subsequent development by Lehn¹⁷ of a discipline which he was later to popularize under the banner of supramolecular chemistry.¹⁸ As this field of small molecule recognition and self-assembly started to unfold, Cram¹⁹ launched a research program under the umbrella of host–guest chemistry²⁰ wherein he investigated²¹ the binding between primary alkylammonium (RNH_3^+) ions and crown ethers in the constitutional range from [18]crown-6 up to [20]crown-6 derivatives. The face-to-face complexes formed between RNH_3^+ ions and these crown ethers are stabilized by strong $[\text{N}^+ \cdots \text{H} \cdots \text{O}]$ hydrogen bonds in addition to dipole–dipole interactions. Eventually in 1995, it was discovered independently in our laboratories,²² as well as in those of Busch²³ that, by increasing the size of the crown ether to a [24]crown-8 constitution, e.g., dibenzo[24]crown-8 (DB24C8), threading of secondary dialkylammonium (R_2NH_2^+) ions through the center of the larger macrocyclic polyether becomes a possibility. This discovery led to the template-directed synthesis²⁴ of numerous rotaxanes and catenanes (i) by threading-followed-by-stoppering²⁵ and (ii) by slippage.²⁶ Then, subsequently in 2001, we uncovered an extremely facile and efficient synthesis of a [2]rotaxane using a clipping approach.²⁷ The outcome, when employing bis(3,5-dimethoxybenzyl)ammonium ions as the source of templating $-\text{CH}_2\text{NH}_2^+\text{CH}_2-$ centers, is a very rapid and efficient formation of a macrocyclic diimine with a [24]crown-8 constitution when 1.0 equiv each of 2,6-pyridinedicarboxaldehyde (**44**) and tetraethylene glycol bis(2-amino-phenyl)ether (**45**) is added to a MeCN solution of the dumbbell at room temperature. This thermodynamically driven self-assembly process²⁸ is stabilized by a number of noncovalent bonding interactions including $[\text{N}^+ \cdots \text{H} \cdots \text{X}]$ hydrogen bonds and $[\text{N}^+ \cdots \text{C} \cdots \text{H} \cdots \text{X}]$ ($\text{X} = \text{O}$ or N) interactions, as well as by $[\pi \cdots \pi]$ stacking interactions between the dumbbell and ring components of the [2]rotaxane. 2,5-Diformylfuran has also been shown²⁹ to be a suitable clipping partner, resulting in enhanced templation, since the O atom in furan is a better hydrogen bond acceptor than the N atom in pyridine, even though the [2]rotaxane formation is considerably slower.

Polyrotaxanes, including main-chain-type,³⁰ poly[n]-rotaxanes,³¹ and cross-linked³², have been at the forefront³³ of polymer and related materials-science research for more than two decades now. The discovery^{28,29} of the highly efficient clipping protocol made it feasible for us to prepare a series of higher-order main-chain polyrotaxanes. Our strategy involves the syntheses of a series of dumbbells which contain a discrete number of $-\text{CH}_2\text{NH}_2^+\text{CH}_2-$ recognition sites spaced evenly from one another along the rod section of the dumbbells. Employing iterative reaction sequences, a series of dumbbells consisting of $n\text{-C}_6\text{H}_4\text{-CH}_2\text{NH}_2^+\text{CH}_2\text{-C}_6\text{H}_4-$ recognition sites were prepared³⁴ with 3,5-dimethoxyphenyl groups serving as stoppers. Addition of the dialdehyde **44** and diamine **45** (n equiv each)

results in the formation of a series of [n]rotaxanes ($n = 2 - 11$) in less than 1 h at room temperature. Computational investigations^{33g} lead one to believe that these oligorotaxanes assume flexible conformations in solution, behaving as randomly assembled coils. This conformation hampers drastically the potential of these molecules to serve as energy transport mediators, for example. We, therefore, have become very interested in controlling the overall conformation of such oligorotaxanes, *i.e.*, making them rigid and rod-like. We reasoned that $[\pi \cdots \pi]$ stacking interactions between adjacent rings would not only provide added stability to the oligorotaxanes, improving the efficiency of the clipping reaction, but would also lend linearity and rigidity to the molecules, rendering them rod-like. Specifically, we rationalized (Figure 1) that placing $n\text{-CH}_2\text{NH}_2^+\text{CH}_2-$ recognition

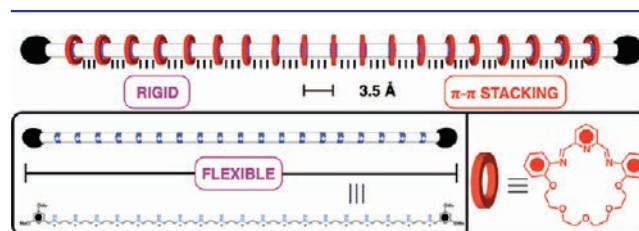


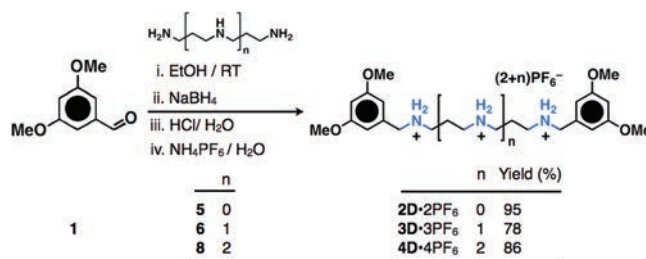
Figure 1. Design of rigid rod-like polyrotaxanes based on $[\pi \cdots \pi]$ stacking interactions between aromatic rings separated by 3.5 Å.

sites approximately 3.5 Å apart from one another in the dumbbell components of the oligorotaxanes would position the rings so as to optimize their inter-ring $[\pi \cdots \pi]$ stacking interactions. Although we have shown³⁵ that this approach is effective in preparing rod-like [n]rotaxanes ($n = 2 - 8$), the production of well-defined, homogeneous, higher-order polyrotaxanes has continued to be a challenge to us as synthetic chemists because it (i) requires the synthesis of dumbbell templates with a well-defined number of recognition sites and (ii) relies upon the successful and efficient condensations of $2n$ components. Herein, we report a detailed investigation (i) of the efficient syntheses of two series of oligorotaxanes **R** and **R'**, (ii) on the profound effect that the distance between the $-\text{NH}_2^+$ recognition sites has on the kinetics and thermodynamics of rotaxane formation, and (iii) of the positive cooperativity that is present in the formation of the **R** series of oligorotaxanes and absent in the **R'** series.

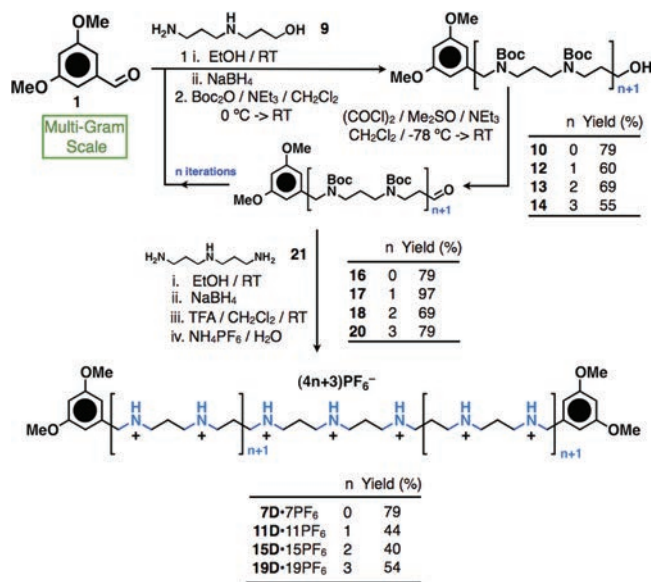
RESULTS AND DISCUSSION

In the beginning we focused our efforts on the synthesis of the shorter oligoammonium dumbbells which involved (Scheme 1)

Scheme 1. Synthesis of the Dumbbells 2D·2PF₆[−], 3D·3PF₆[−], and 4D·4PF₆[−] by the Reductive Amination of 3,5-Dimethoxybenzaldehyde (**1**) and Amino Compounds **5**, **6**, and **8**, Respectively



Scheme 2. Synthesis of the Dumbbells 7D·7PF₆, 11D·11PF₆, 15D·15PF₆, and 19D·19PF₆, Employing Iterative Reaction Sequences



reductive amination between 3,5-dimethoxybenzaldehyde (**1**) and the appropriate amine **5**, **6**, or **8**. Protonation of every secondary amino group along the dumbbell with HCl, followed by counterion exchange, afforded the dumbbells **2D·2PF₆**, **3D·3PF₆**, and **4D·4PF₆**. (Throughout the remainder of this manuscript, the dumbbell components will be designated as **nD·nPF₆**, where *n* is equal to the number of $-\text{CH}_2\text{NH}_2^+\text{CH}_2-$ recognition sites.) The primary challenge we faced in our goal toward preparing a monodisperse [20]rotaxane was the development of the synthetic methodology to prepare longer dumbbells with up to 19 secondary dialkyl-ammonium recognition sites. Along these lines, we employed a protocol (Scheme 2) where by one end (stopper) of the dumbbell was extended in a stepwise fashion. The first iteration started with the reductive amination of 3,5-dimethoxybenzaldehyde (**1**) and diamine **9** to provide a diamino-alcohol which was chemoselectively Boc protected, affording the alcohol **10**. Although several oxidants were screened in the next step, i.e., PCC, IBX, Dess-Martin, and Ley oxidation, they all led to poor conversion or decomposition of the starting material. Swern oxidation, on the other hand, afforded the corresponding aldehyde **16** in good yield. In order to extend the length of the dumbbell precursor, aldehyde **16** was subjected to one, two, or three further iterations of the above reaction sequence to afford the extended aldehydes **17**, **18**, and **20**, respectively. Each of the extended aldehydes was soluble in most organic solvents and they were prepared on a multigram scale. In the last step of the reaction sequence, the aldehydes **16**, **17**, **18**, and **20** were subjected in turn to reductive amination, in a one-pot reaction procedure, with bis(3-aminopropyl)amine (**21**), followed by an acid-mediated global deprotection of the amino groups with TFA and counterion exchange, affording the polyammonium dumbbells **7D·7PF₆**, **11D·11PF₆**, **15D·15PF₆**, and **19D·19PF₆**. Each of these polyammonium salts were isolated in good yield, given the number of functional group manipulations carried out in one pot, as pure compounds without the need for chromatography. In contrast with some other not dissimilar oligoammonium dumbbell components which are poorly soluble,³⁰ **2D·2PF₆**–**19D·19PF₆** are highly soluble in

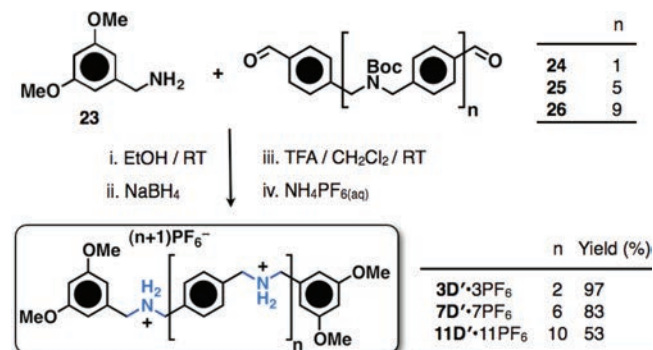
polar organic solvents such as acetone, acetonitrile, and nitromethane, and partially soluble in the less polar dichloromethane.

We also prepared a series of oligoammonium dumbbells which have a *p*-phenylene unit inserted between each of the $-\text{CH}_2\text{NH}_2^+\text{CH}_2-$ recognition sites. These templates would ultimately give rise to a series of oligorotaxanes which serve as control compounds against cooperative effects and conformation. The stepwise syntheses of the oligomeric dumbbells was performed (Scheme 3) by the condensation of benzylamine with benzaldehyde derivatives. In the synthesis of **nD'·nPF₆**, 3,5-dimethoxybenzylamine (**23**) (2 equiv), and the diformyl-terminated oligomers (**24**, **25**, and **26**) (1 equiv), which contain a well-defined number of Boc-protected dialkylamine functions, were condensed, affording the corresponding imines. The imine functions were reduced to the corresponding dialkylamino groups with NaBH₄, and subsequent treatment with TFA resulted in removal of all the Boc protecting groups, affording **nD'·nPF₆** after counterion exchange with an aqueous solution of saturated NH₄PF₆.

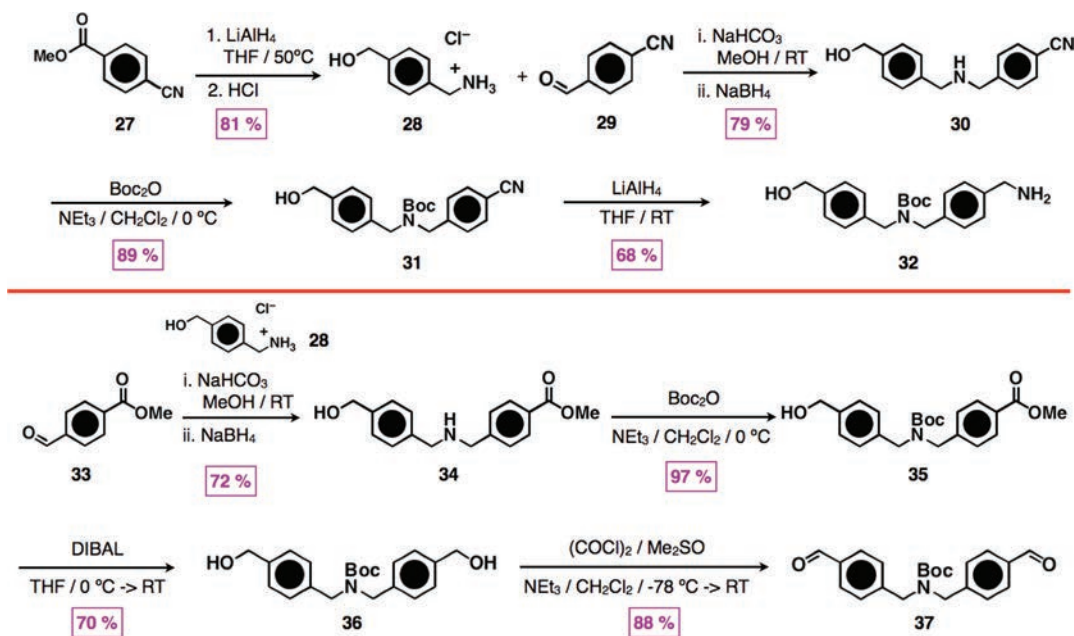
The syntheses of the oligo-*p*-phenylene dumbbells utilizes the diformylated component **37** and the primary amine **32** as the key building blocks. The synthesis (Scheme 4) of **32** was initiated with the reduction of methyl 4-cyanobenzoate (**27**). [4-(Aminomethyl)phenyl]methanol hydrochloride (**28**) was then reacted with 4-formylbenzoxonitrile (**29**) in the presence of NaHCO₃ to form the imine which was reduced with NaBH₄ to afford dialkylamine **30**. The amino functionality was protected with Boc₂O and further reduction of the nitrile with LiAlH₄ provided the building block **32**. The diformyl building block **37** was synthesized employing a similar synthetic protocol, beginning with reductive amination of methyl 4-formylbenzoate (**33**) and **28**, affording the dialkylamine **34** which was subsequently Boc protected. Reduction of the methyl ester with DIBAL and oxidation of each of the alcohols in **36** afforded **37**.

Condensation (Scheme 5) of **37** with the primary amine **32** and subsequent reduction to the dialkylamine affords **38** in 85% yield. The amino functions were chemoselectively Boc-protected, and the resulting diol **40** was subjected to Swern oxidation, affording the diformyl-terminated oligomer **42**, consisting of five Boc-protected amino functions, and serving as the precursor for the dumbbell component **7D'·7PF₆**. Alternatively, **42** can be subjected to a further iteration of the above reaction sequence, beginning with reductive amination with **32**, to afford the diformyl oligomer **43**, consisting of nine Boc-protected amino functions, which ultimately leads to the preparation of **11D'·11PF₆**.

Scheme 3. Synthesis of the Oligomeric Dumbbells 3D'·3PF₆, 7D'·7PF₆, and 11D'·11PF₆ from Dialdehydes 24, 25, and 26, Respectively, and 3,5-Dimethoxybenzylamine (23)



Scheme 4. Syntheses of the Building Blocks 32 and 37, Starting from 27 and 33, Respectively



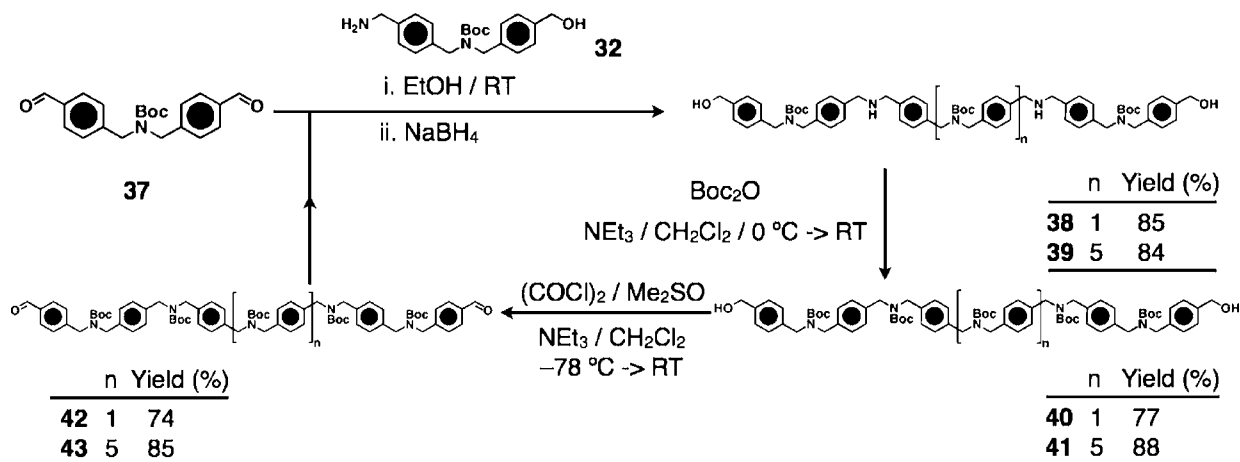
With both series of oligoammonium dumbbells in hand, we turned our attention toward the syntheses of the corresponding oligorotaxanes. Beginning with the rigid series **R**, each of the clipping reactions were performed in 0.75 mL of CD₃CN and monitored by ¹H NMR spectroscopy. (The rotaxanes are designated as *nR*·*n*PF₆, where *n* is equal to the number of –CH₂NH₂⁺CH₂– recognition sites.) The [3]rotaxane **2R**·2PF₆ is produced quantitatively (Figure 2a), on adding a solution containing the dialdehyde **44** and diamine **45** (2 equiv each) to a solution of the bisammonium salt **2D**·2PF₆ in CD₃CN within 5 min of mixing the starting materials together. The chemical shifts of the peaks associated with the imine (H_c), pyridyl (H_a and H_b), and *ortho*-aryl (H_d–H_e) protons of a similar [2]-rotaxane that was prepared²⁷ previously are in good agreement, and as expected, there is only a single set of resonances in the ¹H NMR spectrum for the two homotopic rings encircling (Figure 2b) the dumbbell component. The constitution of the [3]rotaxane was confirmed by the presence of an intense base peak in the electrospray ionization (ESI) mass spectrum at *m/z* 1471.6220, corresponding to [2R·PF₆]⁺. The [3]rotaxane was

isolated (General Procedure I in the Experimental Section) in 93% yield as a yellow powder by layering *i*Pr₂O onto a solution of **2R**·2PF₆ in CD₃CN and collecting the precipitate by filtration.

The [4]rotaxane was also prepared (Figure 3a) in almost quantitative yield by addition of **3D**·3PF₆ to a solution of the dialdehyde **44** and diamine **45** (3 equiv each) in CD₃CN. The ¹H NMR spectrum shows (Figure 3b) two sets of resonances in a relative ratio of 2:1 as a result of the two homotopic outer rings which are heterotopic with respect to the inner ring. Pure **3R**·3PF₆ was isolated in 90% yield and the ESI-MS of this yellow powder confirmed the constitution of the [4]rotaxane with intense base peaks being observed at *m/z* 2149.8608 ([**3R**·2PF₆]⁺), 1002.4507 ([**3R**·PF₆]²⁺), and 619.9806 ([**3R**]³⁺). The [5]rotaxane, **4R**·4PF₆, was prepared in a manner similar to that of **3R**·3PF₆, and the spectroscopic evidence (see SI and Table 1), ¹H NMR spectroscopy and ESI-MS, is consistent with the rotaxane having a rigid and linear conformation.

Having established that the clipping protocol provides an effective means of producing lower-order oligorotaxanes,

Scheme 5. Syntheses of the Bisformyl-Terminated Oligomers 42 and 43 Employing Iterative Reaction Sequences



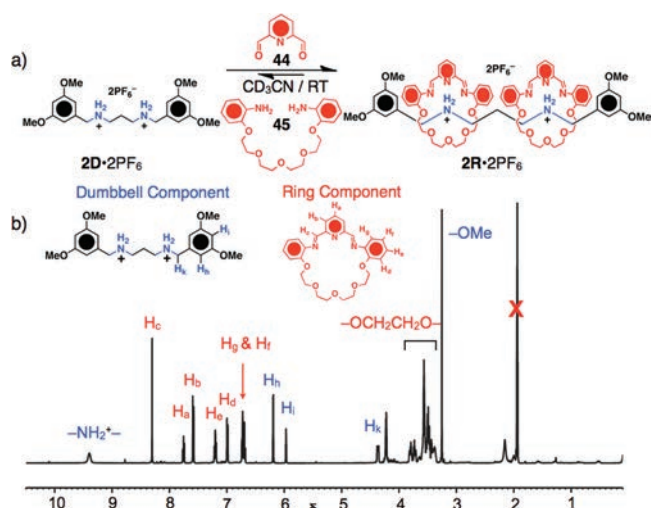


Figure 2. (a) Template-directed synthesis of the [3]rotaxane, $2R \cdot 2PF_6$, starting from $2D \cdot 2PF_6$, 44, and 45. (b) The 1H NMR spectrum (500 MHz, CD_3CN , 298 K) of the [3]rotaxane. The assignments of the resonances are portrayed by partitioning the structural formula of $2R^{2+}$ into its separate dumbbell and ring components.

namely $2R^{2+}$, $3R^{3+}$, and $4R^{4+}$, we turned our attention toward the syntheses (Scheme 6) of higher-order oligorotaxanes with up to 19 rings. Again, in all cases, clipping reactions were performed in 0.75 mL of CD_3CN by mixing together the dumbbell (template) with a dynamic combinatorial library consisting of n equiv (n = number of $-CH_2NH_2^+CH_2-$ recognition sites) of both the diamine 44 and the dialdehyde 45. The resulting golden-yellow solutions were then monitored by 1H NMR

spectroscopy until equilibrium was reached (Table 1) in each case. The spectrum of the [8]rotaxane, $7R \cdot 7PF_6$, consists of four resonances in a 2:2:2:1 ratio in the region around $\delta = 8.00$ ppm for the imine protons of the rings. This observation can be explained by the presence of three homotopic pairs of heterotopic rings (R_A , R_B , and R_C), plus the central heterotopic ring (R_D). Furthermore, the chemical shifts of the imine protons move upfield as they become more shielded toward the center of the [8]rotaxane, *i.e.*, the imine signal arising from R_A appears the furthest downfield ($\delta = 8.19$ ppm), while the imine resonance corresponding to R_D , appears the furthest upfield ($\delta = 7.97$ ppm). The incredible efficiency of the clipping protocol in this case is reflected by the 94% isolated yield which correlates with a 99.6% conversion efficiency for each imine bond formed in the reaction. The ESI-MS of $7R \cdot 7PF_6$ confirms the structural identity of the [8]rotaxane.

Formation of the [12]-, [16]-, and [20]rotaxanes required 10, 12, and 14 h at room temperature, respectively, for the reactions to reach thermodynamic equilibrium. As the lengths of the oligorotaxanes become longer and longer, they begin to resemble polymers, a structural feature which is reflected (Figure 4) by the broadened peaks in the 1H NMR spectra, although, it should be noted that they are in fact discrete, monodisperse products. Their formation can still be confirmed by examining the chemical shifts and relative intensities of the imine resonances. The spectrum of $11R \cdot 11PF_6$, for example, displays four distinct imine resonances which integrate in a 4:4:4:10 ratio. The three homotopic pairs of heterotopic rings nearest the stoppers (R_A , R_B , and R_C) are shielded the least and as a result the corresponding imine protons resonate at lower field ($\delta = 8.18$, 8.02, and 7.97 ppm, respectively). The more

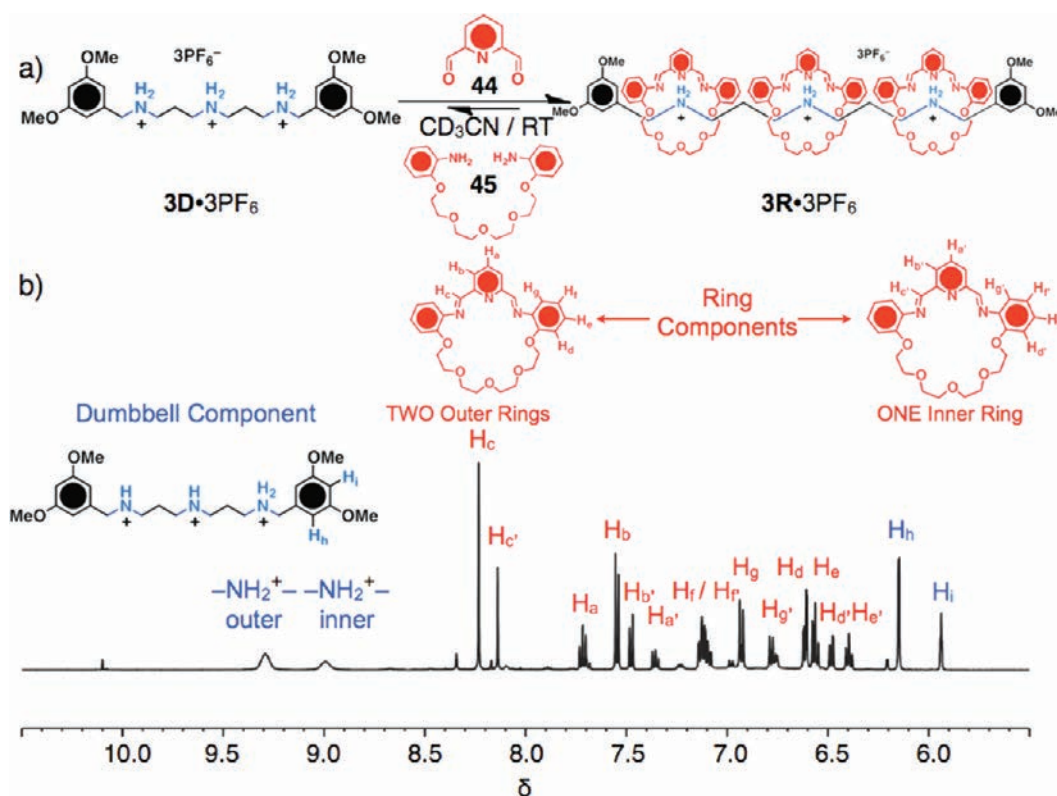
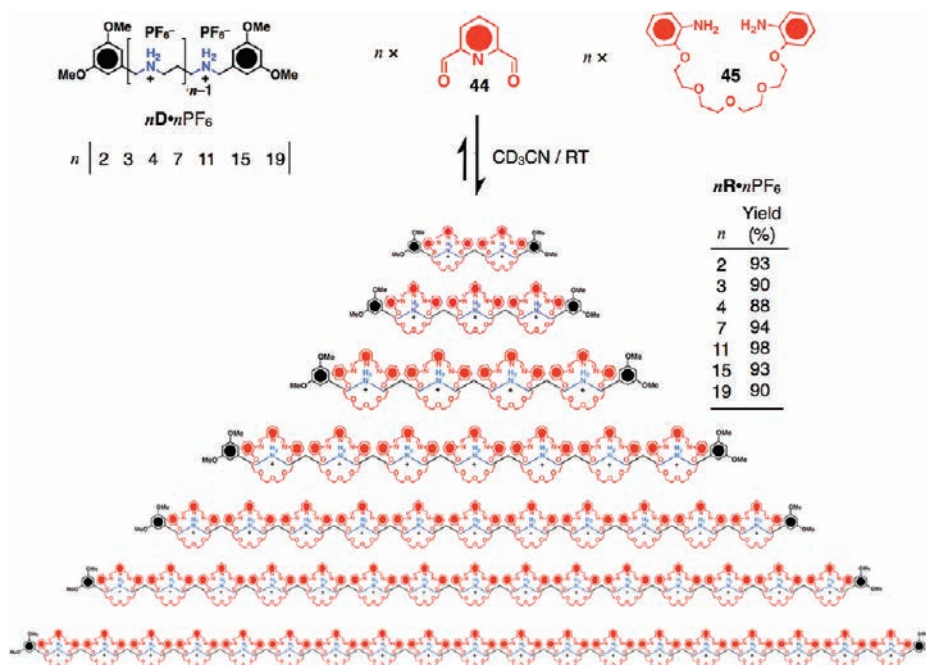


Figure 3. (a) Template-directed synthesis of the [4]rotaxane, $3R \cdot 3PF_6$, starting from $3D \cdot 3PF_6$, 44, and 45. (b) The 1H NMR spectrum (500 MHz, CD_3CN , 298 K) of the [4]rotaxane. The assignments of the resonances are portrayed by partitioning the structural formula of $3R^{3+}$ into its separate dumbbell and ring components.

Table 1. Numbers of Rings, Components, and Imine Bonds Formed in the Case of $nR \cdot nPF_6$, Alongside Characteristic Peaks Observed in Their Respective Mass Spectra^a

compound no.	[<i>n</i>] rotaxane	rings	no. of components ^b	no. of imine bonds	time to reach equilibrium ^c	isolated yield (%) ^d	yield per imine bond (%) ^e	molecular weight (g/mol)	observed ESI-MS signals (m/z) ^f
2R ²⁺	3	2	5	4	<5 min	93	98.2	1617	1471.6220 [M - PF ₆] ⁺
3R ³⁺	4	3	7	6	<5 min	90	98.3	2296	2149.8608 [M - PF ₆] ⁺ 1002.4507 [M - 2PF ₆] ²⁺ 619.9806 [M - 3PF ₆] ³⁺
4R ⁴⁺	5	4	9	8	<5 min	88	98.4	2975	1341.5625 [M - 2PF ₆] ²⁺ 846.0558 [M - 3PF ₆] ³⁺
7R ⁷⁺	8	7	15	14	6 h	94	99.6	5011	1524.2985 [M - 3PF ₆] ³⁺ 1106.9836 [M - 4PF ₆] ⁴⁺ 856.5903 [M - 5PF ₆] ⁵⁺
11R ¹¹⁺	12	11	23	22	10 h	98	99.9	7725	1786.2763 [M - 4PF ₆] ⁴⁺ 1400.0153 [M - 5PF ₆] ⁵⁺ 1142.5061 [M - 6PF ₆] ⁶⁺ 958.5858 [M - 7PF ₆] ⁷⁺
15R ¹⁵⁺	16	15	31	30	12 h	93	99.8	10439	1942.8957 [M - 5PF ₆] ⁵⁺ 1595.9068 [M - 6PF ₆] ⁶⁺ 1346.3478 [M - 7PF ₆] ⁷⁺ 1014.9535 [M - 9PF ₆] ⁹⁺ 898.9877 [M - 10PF ₆] ¹⁰⁺
19R ¹⁹⁺	20	19	39	38	14 h	90	99.7	13154	1734.1194 [M - 7PF ₆] ⁷⁺ 1499.1830 [M - 8PF ₆] ⁸⁺ 1316.6811 [M - 9PF ₆] ⁹⁺ 1170.5047 [M - 10PF ₆] ¹⁰⁺ 1050.6512 [M - 11PF ₆] ¹¹⁺

^aThe isolated yield and yield per imine bond formed indicate the high efficiency and precision of the clipping reaction. ^bThe number of components is determined for $nR \cdot nPF_6$ by $2n + 1$ where n = number of equivalents of **44** or **45**. ^cEquilibrium times were determined by monitoring the clipping reaction by ¹H NMR spectroscopy until no changes in the spectra were observed. ^dAll clipping reactions were performed at room temperature according to General Procedure I in the Experimental Section. ^eThe percent yield for each imine bond formed can be calculated by $(Y)^{1/x}$ where Y = percent yield of $nR \cdot nPF_6$ /100 and x = number of imine bonds formed. ^fHigh-resolution electrospray ionization mass spectra were collected on purified samples of $nR \cdot nPF_6$ redissolved in MeCN.

Scheme 6. Clipping Approach to the Template-Directed Syntheses of the Dynamic Oligorotaxanes $nR \cdot nPF_6$ from the Oligoammonium Templates $nD \cdot nPF_6$ with n equiv Each of **44 and **45**^a**

^aThe oligorotaxanes are structurally rigid on account of extended $[\pi \cdots \pi]$ stacking interactions between contiguous rings which are separated by 3.5 Å. These interactions also assist in the formation of contiguous rings along the backbone of the rotaxane resulting in extremely high conversion efficiencies, up to 99.9%, for each imine bond.

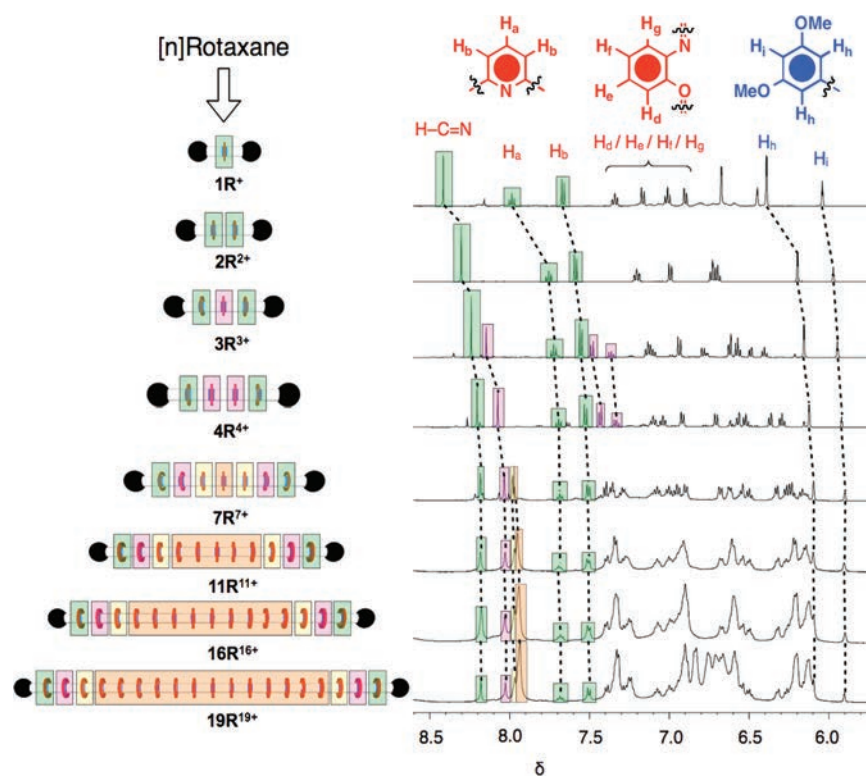


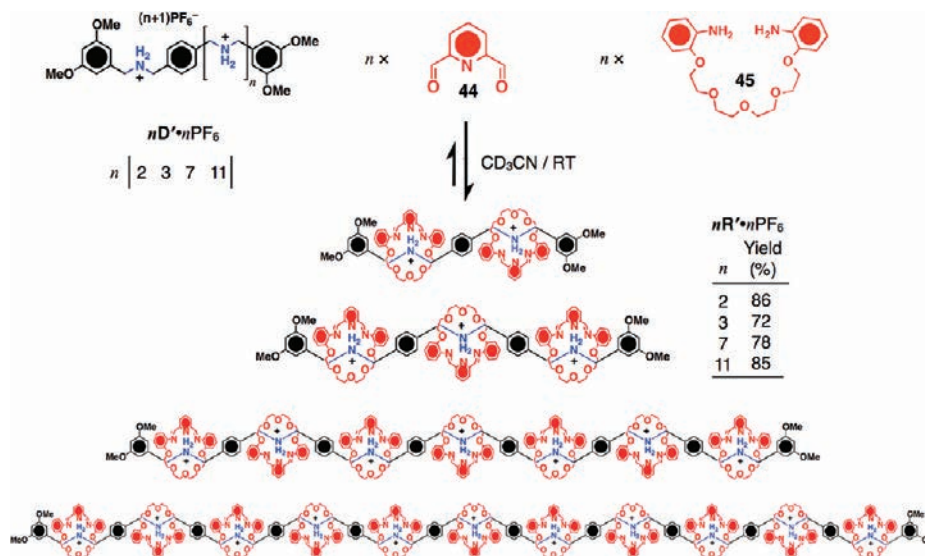
Figure 4. Partial ^1H NMR spectra (500 MHz, CD_3CN , 298 K) of the series of oligorotaxanes showing how the resonances for the imine ($\text{H}-\text{C}=\text{N}$) and aromatic protons (H_a/H_b and H_h/H_i) move to higher fields and, in the case of the benzo ring protons ($\text{H}_c/\text{H}_d/\text{H}_e/\text{H}_f/\text{H}_g$), fan out as more rings are added on going from the [2]rotaxane up to the [20]rotaxane. These chemical shift changes are indicative of multiple $[\pi\cdots\pi]$ stacking interactions.

central of the rings ($R_D - R_F$), which experience the most amount of shielding, share very similar chemical environments and resonate at roughly the same frequencies ($\delta = 7.95$ ppm). It is important to note the amazing efficiencies of the multiple clipping reactions involving 23 components, in the case of the [12]rotaxane, whereby each and every recognition unit along the dumbbell templates the formation of a ring. Moreover, we do not detect any traces of the dumbbell that is not fully saturated with rings, that is, consisting of 10 or fewer rings. Furthermore, an isolated yield of 98% for **11R**·11PF₆ corresponds to a 99.9% conversion efficiency per imine condensation!

The same behavior is observed in the ^1H NMR spectra of the [16]rotaxane **15R**·15PF₆, and also the [20]rotaxane **19R**·19PF₆, wherein the three homotopic pairs of heterotopic rings nearest the stoppers (R_A , R_B , and R_C) are well resolved with the ratios as determined by integration, for **15R**·15PF₆, being 4:4:4:18 where the resonances for the central rings overlap extensively. The difference between the outermost rings of these two oligorotaxanes is expressed by the imine protons. In the clipping reactions with $(n - 1)$ equiv each of **44** and **45**, full conversions to the saturated $[n]$ rotaxane is observed. As was the case with the shorter oligorotaxanes, we have looked for the presence of the dumbbell templates that are not fully saturated, i.e., **19R**¹⁹⁺ with fewer than 19 rings, but do not observe any traces of them by ESI-MS or diffusion-ordered spectroscopy (DOSY). The isolated yields of **15R**·15PF₆ and **19R**·19PF₆ are 93 and 90% which translates to 99.8 and 99.7% conversion per imine bond formed, respectively, during the clipping reactions. By way of a comparison, Grubbs and co-workers³⁶ have described very recently an efficient one-pot synthesis of polyrotaxanes, employing a supramolecular monomer consisting of a polymerizable ammonium salt and crown ether in combination with

dynamic acyclic diene metathesis (ADMet) polymerization. Although this protocol provides a facile procedure for the preparation of polyrotaxanes, it suffers from producing polymers with relatively high polydispersity indices (PDIs) with a maximum of only 82% threading of the rings onto the recognition sites.

The second series of oligorotaxanes which have been designed to prevent $[\pi\cdots\pi]$ stacking interactions between adjacent rings by inserting a *p*-phenylene spacer between each of the $-\text{CH}_2\text{NH}_2^+\text{CH}_2-$ recognition sites, was prepared (Scheme 7) in an analogous fashion. Clipping reactions were conducted in CD_3CN by mixing together the dumbbell templates $n\text{D}'\cdot n\text{PF}_6$ with n equiv each of compounds **44** and **45** and monitoring (Table 2) the reaction mixtures by ^1H NMR spectroscopy. The spectrum (Figure 5) of the [3]rotaxane, **2R'**·2PF₆, which looks very similar to that of **2R**·2PF₆, shows a single set of resonances for the two homotopic rings. However, unlike the spectra of the rotaxanes in the **R** series which were discussed previously, the spectra of the [4]-, [8]-, and [12]rotaxanes, **3R'**·3PF₆, **7R'**·7PF₆, and **11R'**·11PF₆, consist of only two sets of resonances for the imine protons of the rings, the ratios between the two sets of signals calculated by integration of the spectra being 2:1, 1:2.5, and 1:4.5, respectively. This observation can be explained in terms of the heterotopic environments of the rings surrounding the dumbbells whereby the two homotopic rings adjacent to the stoppers (R_A) in the [4]rotaxane are heterotopic with respect to the central ring (R_B). In the [8]rotaxane, however, rings R_B and R_C share very similar chemical environments ($\delta = 8.09$ ppm) but differ from that of R_A ($\delta = 8.26$ ppm). The same is true of R_B , R_C , and R_D ($\delta = 8.08$ ppm) in the [12]rotaxane. The slight difference between rings R_B and R_C is even expressed in the separation of the peaks for the imine protons ($\text{H}-\text{C}=\text{N}$). The crucial difference between this set of spectroscopic data

Scheme 7. Clipping Approach to the Template-Directed Syntheses of the Dynamic Oligorotaxanes $nR'nPF_6$ from the Oligoammonium Templates $nD'nPF_6$ with n equiv Each of 44 and 45

and the spectra for the **R** series is that the resonances of the aromatic protons belonging to $2R^{2+}$, $3R^{3+}$, $7R^{7+}$, and $11R^{11+}$ do not shift as a function of the number of rings encircling the dumbbells. In fact, with the exception of the rings (R_A) closest to the stoppers, each remaining ring finds itself in very similar chemical environments, as reflected by the fact that only two sets of resonances appear in the 1H NMR spectra. This observation is a clear indication that adjacent rings are not close enough to participate in $[\pi \cdots \pi]$ stacking interactions, which suggests that the $[n]$ rotaxanes are much more flexible than $2R^{2+}$ – $19R^{19+}$.

It is worthy to note that the different constitutions of the dumbbells in the **D** and **D'** series have a pronounced effect on the kinetics and thermodynamics of the clipping reactions. For example, under very similar reaction conditions, the [8]- and [12]rotaxanes $7R' \cdot 7PF_6$ and $11R' \cdot 11PF_6$ form in >98% conversion efficiencies in approximately 20–30 min whereas the [8]- and [12]rotaxanes $7R \cdot 7PF_6$ and $11R \cdot 11PF_6$ require 6

and 10 h, respectively, to reach thermodynamic equilibrium with conversions in excess of 99.8%. The interplay between kinetics and thermodynamics in the formation of rotaxanes in the **R** and **R'** series is all too familiar: the more stable the products, the longer it takes for them to be formed. The conversion efficiency for each imine bond formation in the clipping reactions to afford the **R'** rotaxanes range from 94.7 to 99.3%, while the lowest conversion per imine bond formed in the **R** rotaxanes is 98.2% and reaches up as far as 99.9% for $11R \cdot 11PF_6$. The increased efficiency of production within the **R** series compared with the **R'** series could be the result of an additional templation effect, wherein formation of one ring can template the formation of a contiguous ring by, presumably, stabilizing extended $[\pi \cdots \pi]$ stacking interactions. Although this difference may not seem to be significant, it is actually highly relevant when it comes to producing good yields of high molecular weight compounds. The clipping reactions that are taking place along the dumbbells may be likened to a step-growth polymerization

Table 2. Numbers of Rings, Components, and Imine Bonds Formed in the Case of $nR'nPF_6$, Alongside Characteristic Peaks Observed in Their Respective Mass Spectra

compound no.	$[n]$ rotaxane	no. of rings	no. of components ^a	no. of imine bonds	time to reach equilibrium ^b	isolated yield (%) ^c	yield per imine bond (%) ^d	molecular weight (g/mol)	observed ESI-MS signals (m/z) ^e
$2R^{2+}$	3	2	5	4	<5 min	86	96.3	1680	1533.6300 $[M - PF_6]^+$ 1387.6610 $[M - HPF_6 - PF_6]^+$ 694.3370 $[M - 2PF_6]^{2+}$
$3R^{3+}$	4	3	7	6	<5 min	72	94.7	2420	2127.9460 $[M - HPF_6 - PF_6]^+$ 1064.4621 $[M - 2PF_6]^{2+}$ 661.3218 $[M - 3PF_6]^{3+}$
$7R^{7+}$	8	7	15	8	20 min	78	98.2	5383	1648.3245 $[M - 3PF_6]^{3+}$ 1200.1020 $[M - 4PF_6]^{4+}$ 931.0238 $[M - 5PF_6]^{5+}$
$11R^{11+}$	12	11	23	14	30 min	85	99.3	8346	751.6797 $[M - 6PF_6]^{6+}$ 2428.6179 $[M - 3PF_6]^{3+}$ 1785.3202 $[M - 4PF_6]^{4+}$

^aThe number of components is determined for $nR' \cdot PF_6$ by $2n+1$ where n = number of equivalents of 44 or 45. ^bEquilibrium times were determined by monitoring the clipping reaction by 1H NMR spectroscopy until no changes in the spectra were observed. ^cAll clipping reactions were performed at room temperature according to General Procedure I in the Experimental Section. ^dThe percent yield for each imine bond formed can be calculated by $(Y)^{1/x}$ where Y = percent yield of $nR' \cdot nPF_6/100$ and x = number of imine bonds formed. ^eHigh-resolution electrospray ionization mass spectra were collected on purified samples of $nR' \cdot nPF_6$ redissolved in MeCN.

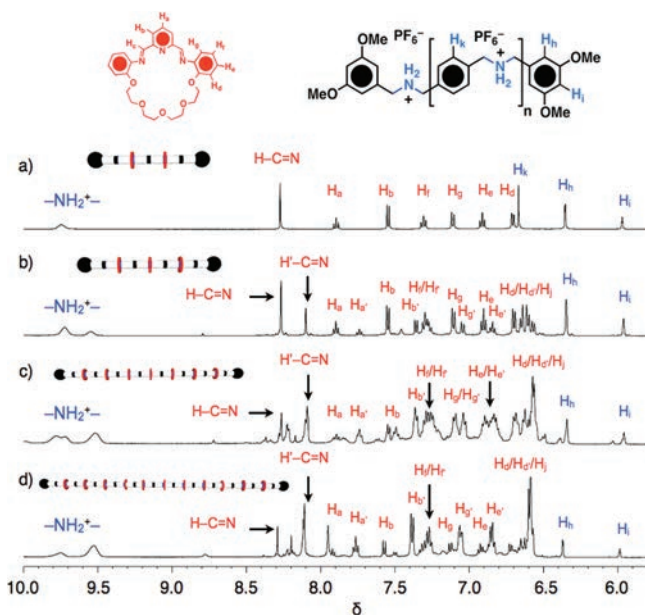


Figure 5. Partial ^1H NMR spectra (500 MHz, CD_3CN , 298 K) of $2\text{R}^+\cdot 2\text{PF}_6^-$, $3\text{R}^+\cdot 3\text{PF}_6^-$, $7\text{R}^+\cdot 7\text{PF}_6^-$, and $11\text{R}^+\cdot 11\text{PF}_6^-$ showing how the resonances for the imine ($\text{H}-\text{C}=\text{N}$) and aromatic protons (H_a/H_b and $\text{H}_d/\text{H}_c/\text{H}_f/\text{H}_g$) do not move to higher field upon the progressive addition of more and more rings. This behavior is a result of the absence of $[\pi\cdots\pi]$ stacking interactions between adjacent rings.

process for which it is well understood that very long linear polymers are generally not attainable since even at 98% conversion per reaction, the degree of polymerization³⁷ (DP) is still only 50. An increase of just 1% (i.e., 99% per reaction), however, gives a DP of 100, while 99.9% conversion per reaction correlates with a DP of 1000. Consequently, the methodology we have developed could potentially be employed for the syntheses of even higher order $[n]$ rotaxanes ($n \geq 50$) as a result of the extended $[\pi\cdots\pi]$ stacking interactions increasing the efficiency of each clipping reaction.

In order to find out if there is a cooperative effect at work during the self-assembly of the oligorotaxanes in the **R** series, we performed an experiment (Figure 6a) in which $2\text{D}\cdot 2\text{PF}_6$ was added to a solution of only 1 equiv each of **44** and **45**. There are three potential outcomes from this experiment, (i) the assembly of the second ring around $2\text{D}\cdot 2\text{PF}_6$ is more favorable than the clipping of the first ring, i.e., there is positive cooperativity³⁸ resulting in the production of 2D^{2+} and 2R^{2+} , (ii) the formation of the second ring is not promoted i.e., there is zero cooperativity, by the presence of the first ring and a statistical mixture arises affording a 1:2:1 ratio of 2D^{2+} : 1R^{2+} : 2R^{2+} , and (iii) the formation of the second ring is prevented, i.e., there is negative cooperativity, by the presence of the first ring and so much more of 1R^{2+} than represented by a statistical mixture is the outcome. In the event, once the dynamic system came to equilibrium, the ^1H NMR spectrum (Figure 6b) revealed that a statistical mixture, scenario (ii), was the result and so it follows that there is no cooperativity operating in this case.

We decided that, although cooperativity is zero in the case of 2D^{2+} , it might start to become positive when there are more than two recognition sites on the dumbbell. We therefore chose to carry out an equilibration involving the formation of the [4]- and [5]rotaxanes. First of all, $3\text{D}\cdot 3\text{PF}_6$ was added (Figure S9a) to a solution of **44** and **45** (1.5 equiv of each). At equilibrium, the ^1H NMR spectrum (Figure S9b) showed 3R^{3+} to be the

major product. Integration of those resonances known to arise from the imines of 3R^{3+} indicated that the [4]rotaxane accounts for 75% of the species present in solution, while the remaining 25% of the mass balance belongs to a combination of 3D^{3+} , 1R^{3+} and 2R^{3+} . All four of these species were identified as their PF_6^- salts in the ESI-MS. A purely statistical mixture wherein no one species is favored thermodynamically would result in the formation of only 17% of the [4]rotaxane. The fact that 3R^{3+} exists in quantities that are more than four times that expected on a statistical basis, is a clear indication that positive cooperativity is at play.

The analogous equilibrium experiment was performed (Figure S10a) in the case of the [5]rotaxane $4\text{R}\cdot 4\text{PF}_6$ by adding 2 equiv each of **44** and **45** to $4\text{D}\cdot 4\text{PF}_6$. Quantitative analysis of the ^1H NMR spectrum (Figure S10b) indicates that 4R^{4+} is present in the reaction mixture at 50% while the remaining 50% consists of 4D^{4+} , 1R^{4+} , 2R^{4+} , and 3R^{4+} . A purely statistical mixture would have afforded only 10% of 4R^{4+} and so the experiment results in five times more of the [5]rotaxane being formed than would be expected on a statistical basis. Additionally, the positive cooperativity appears to be on the rise the more recognition sites there are present on the dumbbell. This increase in positive cooperativity as the **R** series of oligorotaxanes is mounted is consistent with the fact that the conversion per imine bond in each case of the clipping reactions rises (Table 1) from 98.2% in the case of the [3]rotaxane to 99.6% in the [8]rotaxane and then remains more or less constant for the [12]-, [16]-, and [20]rotaxanes in the range of 99.7–99.9%, within experimental error.

Some insights into the conformations adopted by the **R** series of oligorotaxanes can be obtained from a comparison of the ^1H NMR spectra (Figure 4) for $1\text{R}^+ - 19\text{R}^{19+}$. In proceeding from 1R^+ to 2R^{2+} , 3R^{3+} , 4R^{4+} , 7R^{7+} , 11R^{11+} , and 15R^{15+} all of the way up to 19R^{19+} , the resonances for the protons on the rings that are nearest the stoppers of the dumbbells move progressively upfield. The signal for the imine protons on the outermost rings of the [20]rotaxane resonates 0.25 ppm upfield relative to that in the [2]rotaxane. This upfield trend in chemical shifts is also observed for the pyridyl (H_a and H_b) and aryl ($\text{H}_d - \text{H}_i$) protons in the oligorotaxanes. These ^1H NMR spectral characteristics can be explained³⁹ by the cumulative number of $[\pi\cdots\pi]$ stacking interactions as the **R** series of

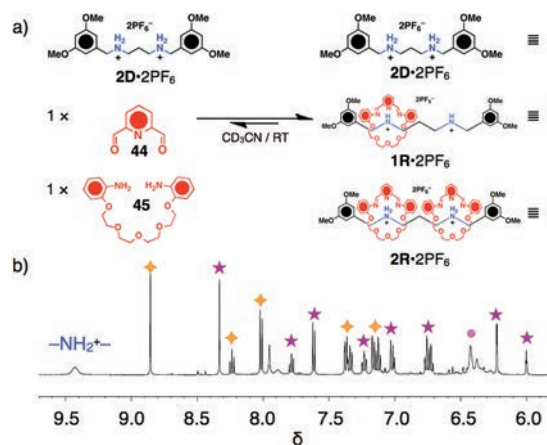


Figure 6. (a) Reaction between $2\text{D}\cdot 2\text{PF}_6$ and 1.0 equiv each of **44** and **45** to probe a potential cooperative effect during the self-assembly process. (b) The partial ^1H NMR spectrum (500 MHz, CD_3CN , 298 K) at equilibrium. The 1:2:1 ratio between 2D^{2+} : 1R^{2+} : 2R^{2+} is indicative of a statistical distribution whereby no one species is favored thermodynamically.

Table 3. Collisional Cross Sections (CCSs) and Drift Times (t_D) Associated with Different Charged States of the [3]-, [4]-, [8]-, and [12]Rotaxanes

compound	m/z	charge	ccs (\AA^2)	t_D (ms)
$2R^{2+}$	1471.63	1	304.31	15.94
	663.33	2	286.65	5.07
$2R^{2+}$	1533.65	1	332.42	18.24
	694.33	2	297.20	5.36
$3R^{3+}$	1002.95	2	375.43	7.68
	620.31	3	382.28	4.26
$3R^{3+}$	1064.97	2	392.45	8.22
	661.68	3	388.57	4.37
	2359.92	2	683.96	19.22
$7R^{7+}$	1524.96	3	641.67	9.42
	1107.48	4	621.11	5.79
	857.00	5	612.70	4.04
	690.04	6	625.54	3.16
	570.72	7	645.18	2.62
$7R^{7+}$	2545.96	2	708.64	20.29
	1649.32	3	661.10	9.86
	1200.76	4	647.49	6.17
	932.62	5	727.82	5.25
	752.19	6	752.97	4.19
	623.87	7	752.28	3.31
	1786.27	4	919.07	10.52
$11R^{11+}$	1400.02	5	897.57	7.23
	1142.53	6	883.45	5.35
	958.01	7	888.04	4.26
	820.66	8	889.29	3.49
	713.37	9	893.71	2.94
	627.53	10	892.55	2.50
	557.30	11	926.76	2.29
	1941.30	4	880.56	9.86
	1524.05	5	869.56	6.89
	1245.87	6	1044.33	6.90
	1047.18	7	1112.57	6.01
$11R^{11+}$	898.17	8	1114.63	4.92
	782.26	9	1121.11	4.15
	689.54	10	1111.50	3.49
	613.67	11	1147.71	3.17

[n]rotaxanes is scaled from $n = 2$ to 20. This realization suggests very strongly to us that the conformations of these oligorotaxanes are rod-like in shape in solution.

For further analysis of the solution state behavior of the oligorotaxanes, ion-mobility mass-spectrometry (IM-MS)⁴⁰ was performed on the [3]-, [4]-, [8]-, and [12]rotaxanes.⁴¹ All compounds were dissolved in MeCN and injected into the instrument using a syringe pump. For all four pairs, namely, $2R^{2+}$ and $2R^{2+}$, $3R^{3+}$ and $3R^{3+}$, $7R^{7+}$ and $7R^{7+}$, and $11R^{11+}$ and $11R^{11+}$, the R' series of oligorotaxanes revealed (Table 3) higher collision cross sections (CCSs) than the oligorotaxanes in the R series. In the cases of the [3]- and [4]rotaxanes, the CCSs decrease with increasing charge on account of the loss of PF_6^- counterions which contribute to the overall size of the molecules. The CCSs are larger for $2R^{2+}$ and $3R^{3+}$ than for $2R^{2+}$ and $3R^{3+}$, respectively, as a result of the bulkier xylene linkers in the dumbbells in the R' series as compared to the propylene linkers in the R series. For the [8]- and [12]rotaxanes, the CCSs initially show the same behavior until they reach a threshold (Figure 7): the removal of five PF_6^- counterions causes a dramatic increase in the CCS of $7R^{6+}$ as compared to the lower charged ions of

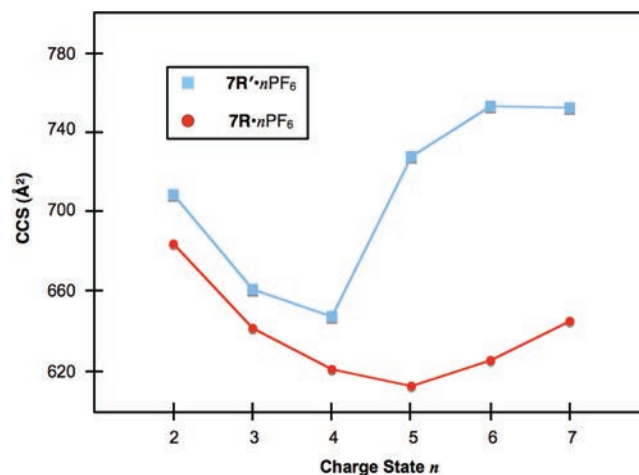


Figure 7. Collisional cross sections (CCSs) for the [8]rotaxanes $7R^{7+}$ and $7R^{7+}$ plotted against the charge state of the ions.

$7R'nPF_6$, while the loss of six PF_6^- counterions results in only a small increase in the CCS for $7R^{6+}$. The same behavior is observed (Figure 8) in the case of the [12]rotaxanes, wherein the removal of six PF_6^- counterions results in a dramatic increase in the CCS of $11R^{6+}$ while the CCSs of $11R'nPF_6$ remain relatively constant throughout the charge state series. The initial decrease in CCSs for both series of the [8]- and [12]rotaxanes can once again be explained by the loss of PF_6^- counterions which contribute to the overall size of the ions. We hypothesize that the counterions play a crucial role in balancing the charge of the oligorotaxanes such that at the beginning of the charge state series, both the R and R' series are roughly the same apparent size. However, as PF_6^- counterions are stripped from the oligorotaxanes, the molecules distort so as to distance the charges along the backbone of the dumbbells as far away from one another as possible. In the case of the R' series of oligorotaxanes, this distortion is manifested in the increase in CCSs. The greater flexibility of the R' oligorotaxanes results in more collisions with the gas molecules in the drift tube and therefore a larger CCS value. On the other hand, the R series of oligorotaxanes do not have the same freedom to “wobble” around as a result of the extended $[\pi \cdots \pi]$ stacking interactions along their backbones. Consequently, fewer collisions occur

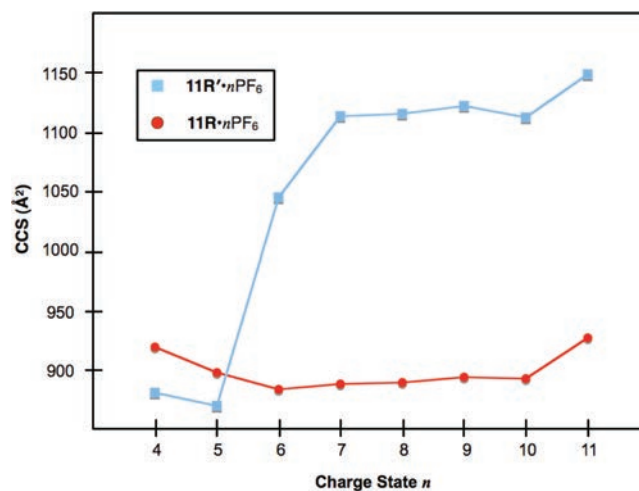


Figure 8. Collisional cross sections (CCSs) for the [12]rotaxanes $11R^{11+}$ and $11R^{11+}$ plotted against the charge state of the ions.

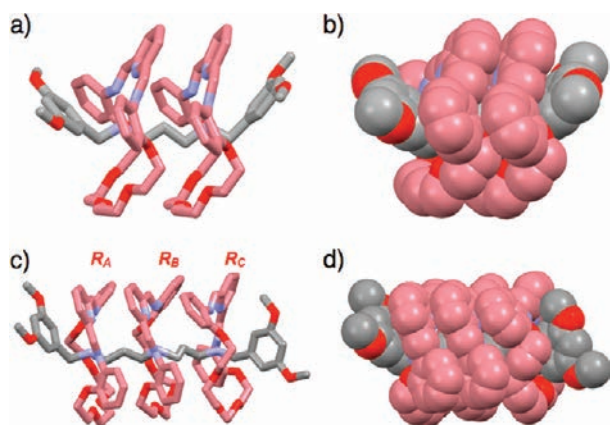


Figure 9. (a) Stick and (b) space-filling representations of the solid-state structure of $2R^{2+}$. The $[N^+-H\cdots N]$ distances range from 2.93 to 3.04 Å between nitrogen atoms and have $[N^+-H\cdots N]$ angles of 172 and 174°. (c) Stick and (d) space-filling representations of the solid-state structure of $3R^{3+}$. Hydrogen atoms and counterions have been omitted and discounted for clarity.

with the gas molecules in the drift tube and we do not observe a significant increase in their CCS values.

Further information on the conformational behavior of the oligorotaxanes can be gleaned from the solid-state structures of the lower order rotaxanes, namely $2R^{2+}$ and $3R^{3+}$. Good quality single crystals suitable for X-ray diffraction analysis were grown by liquid–liquid diffusion of *i*Pr₂O into a solution of $2R\cdot 2PF_6$ in CH_2Cl_2 . The solid-state structure (Figure 9a,b) of $2R^{2+}$ reveals^{42,43} that the three arenes in each of the two rings are in register with one another and their average mean planes in all cases are separated by the optimal $[\pi\cdots\pi]$ stacking distance of 3.5 Å. Importantly, the conformation of $2R^{2+}$ is stabilized by four strong $[N^+-H\cdots N]$ hydrogen bonds ranging between 2.93 and 3.03 Å between nitrogen atoms, plus additional $[\pi\cdots\pi]$ stacking interactions between one of the terminal 3,5-dimethoxyphenyl stoppers on the dumbbell with one of the pyridyl units in one of the rings, all acting in unison to impose a linear rigid conformation on the [3]rotaxane $2R^{2+}$.

X-ray quality single crystals of $3R\cdot 3PF_6$ were also grown by the vapor diffusion of *tert*-butylmethyl ether into a solution of $3R\cdot 3PF_6$ in MeOH. In this case, the solid-state structure (Figure 9 c/d) of $3R^{3+}$ reveals^{42,44} that the arenes in two of the rings (R_A and R_B) are in register with one another, the average mean planes between their stacked arenes are separated by a distance of 3.5 Å, while the third ring (R_C) is out of register with the other two rings (R_A and R_B) by about 52°. The overall message, nonetheless, of rigid rod-like conformations for the molecules remains a forceful one.

In an attempt to shed some additional light on the conformations adopted by these oligorotaxanes which could not be obtained crystalline, a comprehensive molecular mechanics investigation was initiated employing an approach that is an adaptation of previous molecular mechanics studies⁴⁵ on rotaxanes. Initial geometries were generated using coordinates from the crystal structure of $2R\cdot 2PF_6$ as a template and the structures were then minimized using a simulated annealing procedure. Each structure was subjected to a sequence of 100 ps molecular dynamics (MD) simulations using the OPLS2005 force field with an implicit H₂O solvation model starting at 450 K and lowering the temperature in 25 degree increments until 300 K was reached.⁴⁶ The resulting structures were then minimized

further using a 1 ns MD simulation at 300 K. The minimized structures are portrayed in Figure 10.

Molecular mechanics show that the R' series of oligorotaxanes with *p*-phenylene spacers between the $-CH_2NH_2^+CH_2-$ recognition sites tend to adopt quite flexible conformations. Put another way, the rings associated with the monomeric units appear to take up random orientations with respect to each other along the chains, resulting in conformations (Figure 10b) with bends and kinks all of the way along their backbones. This tendency to form flexible conformations was noted³¹ previously when carrying out MD simulations on very similar oligorotaxanes.

In the case of the R series of oligorotaxanes with propylene spacers between the $-NH_2^+$ centers in the $-CH_2NH_2^+CH_2-$ recognition sites, their structures appeared to maintain linear rod-like geometries overall throughout the course of the simulations. The molecules adopt conformations (Figure 10a) with a much higher degree of internal order being expressed between the rings of the repeating monomeric units. It also appears that the extended $[\pi\cdots\pi]$ stacking interactions are conserved along the entire backbone of the oligorotaxanes. This observation is in good agreement with the crystal structures which have already been discussed for $2R^{2+}$ and $3R^{3+}$ in the solid-state. One notable feature revealed by the molecular mechanics on the higher-order rotaxanes is their propensity to become curved in shape as the DP of the oligorotaxanes increases. This phenomenon can be explained by the attraction of the arene residues, one to the other through a combination of multiple hydrophobic and $[\pi\cdots\pi]$ stacking interactions counter balanced by the electrostatic repulsions that must occur between the lone pairs of electrons on the ether oxygen atoms of adjacent polyether loops located on the opposite side of the rod-shaped molecules from the arene residues. Moreover, based on the MD simulations, we are inclined to speculate that polymeric analogues of these oligorotaxanes could potentially form helical arrays on a macroscopic ($\sim 1\ \mu\text{m}$) scale.

All in all, the interplay between the hydrogen bonding and $[\pi\cdots\pi]$ stacking interactions working in unison have proven to effectively promote the self-assembly of oligorotaxanes in a remarkably efficient way. Previously, a monodisperse polyethylene glycol dumbbell (28-mer) was prepared^{30c} and subsequently threaded with α -cyclodextrins (α -CDs) and stoppered affording polyrotaxanes. In this case, a maximum of

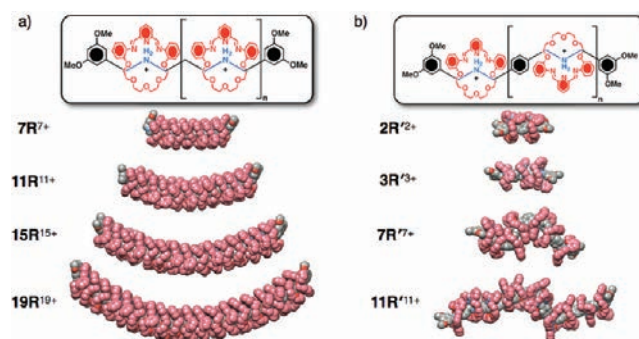


Figure 10. Structures of oligorotaxanes minimized using a simulated annealing procedure. The R' series of oligorotaxanes containing a *p*-phenylene spacer (a) have a considerably less ordered backbone structure than those containing propylene spacer units in the R series of oligorotaxanes (b). The MD simulations indicate that the stacking interactions of nR^{n+} are conserved, even in lengths up to the [20]rotaxane.

only 12 α -CDs were able to be threaded onto the dumbbell. We later showed that a monodisperse [14]rotaxane could be prepared³⁴ by the clipping approach wherein each and every recognition unit along the dumbbell templated the formation of a ring. We were ultimately limited, however, from extending this protocol to the synthesis of higher-order polyrotaxanes on account of the (i) poor solubility, and (ii) drop-off in yields with increasing numbers of rings. Each of these limitations have been remedied in the preparation of the **R** series of oligorotaxanes which are highly soluble and benefit from up to 99.9% conversion efficiencies. These two features combined have allowed us to access a monodisperse [20]rotaxane. Additionally, this methodology appears to be conducive to the construction of even higher-order, monodisperse [*n*]rotaxanes ($n \geq 50$), on account of positive cooperativity.

CONCLUSION

The take-home message from the results described in this full paper is contained in the data summarized in Tables 1 and 2 from which it may be concluded that there are “special forces” at work during the template-directed syntheses of oligorotaxanes in the **R** series (Table 1) that are not evident in the **R'** series (Table 2). It would appear that if orthogonal recognition motifs – in this case, hydrogen bonding orchestrating the clipping of the rings onto the dumbbells with many equally and strategically placed recognition sites augmented by multiple extended stacking interactions by up to three arene units per ring in the **R** series – are introduced into self-assembly processes proceeding or accompanying acts of templation in covalent synthesis, then molecules of high molecular weights can be produced with awesome efficiencies – in this case, oligorotaxanes up to a [20]rotaxane in yields of 90%. In this **R** series of oligorotaxanes, it would appear that progressively enhanced molecular recognition and increased positive cooperativity go hand-in-hand during chemical syntheses. The implication is that a perfect alignment between noncovalent and dynamic covalent synthesis endows template-directed protocols with the ability to create monodisperse multifunctional macromolecules in a remarkably efficient manner at ambient temperature.

EXPERIMENTAL SECTION

Materials and Methods. Anhydrous dichloromethane (CH_2Cl_2) and tetrahydrofuran (THF) were obtained from a SC Water USA Glass Contour Seca Solvent System. Absolute ethanol (EtOH), anhydrous triethylamine (NEt_3), methanol (MeOH), and dimethylsulfoxide (Me_2SO) were purchased from Aldrich and handled under an atmosphere of dry nitrogen. CDCl_3 , CD_2Cl_2 , CD_3CN , and D_2O were purchased from Aldrich and used without further purification. All other reagents were purchased from commercial sources and were employed without further purification. All reactions were carried out under an atmosphere of dry nitrogen in flame-dried flasks using anhydrous solvents, unless indicated otherwise. Thin-layer chromatography (TLC) was carried out using glass plates, pre-coated with silica gel 60 with fluorescent indicator (Whatman LK6F). The plates were inspected by UV light (254 nm) and/or potassium permanganate stain. Column chromatography was carried out by the flash technique using silica gel 60F (230 – 400 mesh). ^1H and ^{13}C NMR spectra were recorded on a Bruker ARX500 (500 MHz) spectrometer. The chemical shifts (δ) for ^1H spectra are given in ppm and referenced to the residual proton signal of the deuterated solvent. The chemical

shifts (δ) for ^{13}C spectra are referenced relative to the signal from the carbon of the deuterated solvent. Abbreviations used to define multiplicities are as follows: s = singlet; d = doublet; t = triplet; q = quartet; m = multiplet; br = broad. High-resolution mass spectra were measured on a Finnigan LCQ iontrap mass spectrometer (HR-ESI).

Synthesis. 2,6-Pyridinedicarboxaldehyde⁴⁷ (**44**) and tetraethylene-glycol bis(2-amino-phenyl)ether⁴⁸ (**45**) were prepared according to literature procedures.

General Procedure A. A solution of 3-(3-aminopropyl-amino)propan-1-ol (**9**) (1.0 equiv) in anhydrous EtOH (0.5 M) was added to a solution of the requisite aldehyde (1.0 equiv) in anhydrous EtOH (0.2 M), and the resulting solution was stirred at room temperature for 16 h. NaBH_4 (2.0 equiv) was added to the reaction mixture, which was stirred for an additional 5 h, before being concentrated in vacuo. The residue was taken up in H_2O (100 mL), extracted with EtOAc (3 \times), dried (MgSO_4), and filtered through a pad of Celite, and the filtrate was concentrated in vacuo to provide the extended diamino alcohol as a yellow oil that was used directly in the next step without further purification.

General Procedure B. Di-*tert*-butyldicarbonate (2.0 equiv) was added dropwise over 5 min to a solution of the diamino alcohol (1.0 equiv of crude oil obtained in the previous step) and NEt_3 (4.0 equiv) in anhydrous CH_2Cl_2 (0.1 M) at 0 $^\circ\text{C}$. The resulting solution was warmed to room temperature gradually and then stirred for 16 h before being concentrated in vacuo. The residue was taken up in EtOAc, and the insoluble salt was removed by filtration. The filtrate was concentration in vacuo and the residue was purified by silica gel flash chromatography to provide typically a yellow viscous oil.

10. Following general procedures A and B (based on 10.0 g of 3,5-dimethoxy-benzaldehyde (**1**)), 22.9 g (79% over two steps) of **10** was isolated (SiO_2 ; $R_f = 0.4$, 50/50 v/v EtOAc in hexanes) as clear viscous oil. ^1H NMR (CDCl_3 , 500 MHz): δ 6.36 (br. s, 3H), 4.36 (br. s, 2H), 3.77 (s, 6H), 3.52 (br. s, 2H), 3.30–3.09 (m, 6H), 1.72 (br. s, 2H), 1.62 (br. s, 2H), 1.48 (s, 9H), 1.43 (s, 9H). ^{13}C NMR (CDCl_3 , 125 MHz): δ 161.1, 156.0, 155.7, 105.7, 105.3, 99.0, 80.0, 58.3, 50.8, 50.3, 45.1, 44.6, 42.6, 30.7, 28.6, 28.5. MS (ESI): m/z Calcd for $\text{C}_{25}\text{H}_{43}\text{N}_2\text{O}_7$ [$M + \text{H}$] $^+$: 483.31, found 483.39; Calcd for $\text{C}_{25}\text{H}_{42}\text{N}_2\text{NaO}_7$ [$M + \text{Na}$] $^+$: 505.29, found 505.33.

12. Following general procedures A and B (based on 8.50 g of the aldehyde **16** in the reductive amination step), 8.30 g (60% over two steps) of **12** was isolated (SiO_2 ; $R_f = 0.3$, 70/30 v/v EtOAc in hexanes) as a yellow viscous oil. ^1H and ^{13}C spectra are provided in the SI. HR-MS (ESI): m/z Calcd for $\text{C}_{41}\text{H}_{73}\text{N}_4\text{O}_{11}$ [$M + \text{H}$] $^+$: 797.5270, found 797.5289; Calcd for $\text{C}_{41}\text{H}_{76}\text{N}_5\text{O}_{11}$ [$M + \text{NH}_4$] $^+$: 814.5536, found 814.5554; Calcd for $\text{C}_{41}\text{H}_{72}\text{N}_4\text{NaO}_{11}$ [$M + \text{Na}$] $^+$: 819.5090, found 819.5100.

13. Following general procedures A and B (based on 6.95 g of the aldehyde **17** used in the reductive amination step), 6.10 g (69% over two steps) of **13** was isolated (SiO_2 ; $R_f = 0.4$, 70/30 v/v EtOAc in hexanes) as a yellow viscous oil. ^1H and ^{13}C spectra are provided in the SI. HR-MS (ESI): m/z Calcd for $\text{C}_{57}\text{H}_{103}\text{N}_6\text{O}_{15}$ [$M + \text{H}$] $^+$: 1111.7476, found 1111.7453; Calcd for $\text{C}_{57}\text{H}_{106}\text{N}_7\text{O}_{15}$ [$M + \text{NH}_4$] $^+$: 1128.7741, found 1128.7743; Calcd for $\text{C}_{57}\text{H}_{102}\text{N}_6\text{NaO}_{15}$ [$M + \text{Na}$] $^+$: 1133.7295, found 1133.7281.

14. Following general procedures A and B (based on 4.20 g of the aldehyde **18** used in the reductive amination step), 2.81 g (55% over two steps) of **14** was isolated (SiO_2 ; $R_f = 0.4$, 70/30 v/v EtOAc in hexanes) as a yellow viscous oil. ^1H and ^{13}C

spectra are provided in the SI. HR-MS (ESI): m/z Calcd for $C_{73}H_{133}N_8O_{19}$ $[M + H]^+$: 1425.9682, found 1425.9634; Calcd for $C_{73}H_{132}N_8O_{19}$ $[M + NH_4]^+$: 1442.9947, found 1442.9931; Calcd for $C_{73}H_{132}N_8NaO_{19}$ $[M + Na]^+$: 1447.9501, found 1447.9508.

General Procedure C. Oxalyl chloride (2.0 equiv per alcohol) was added to a solution of Me_2SO (4.0 equiv) in anhydrous CH_2Cl_2 (0.1 M) at -78 °C, and the resulting solution was stirred for 10 min before a solution of the primary alcohol (1.0 equiv, 0.5 M in anhydrous CH_2Cl_2) was added dropwise. The reaction mixture was stirred for 20 min before adding NEt_3 (4.0 equiv). The reaction mixture was warmed to room temperature gradually over the course of 2 h and allowed to stir for a further 4 h, upon which the reaction was purged with a stream of air for 30 min to reduce significantly the odor of Me_2S during purification steps. The reaction mixture was then concentrated in vacuo. The residue was taken up in EtOAc, and the insoluble salt was removed by filtration. The filtrate was concentrated in vacuo and the residue was purified by silica gel flash chromatography to provide typically a yellow viscous oil.

16. Following general procedure C (based on 10.0 g of **10**), 7.9 g (79%) of **16** was isolated (SiO_2 : $R_F = 0.4$, 60/40 v/v EtOAc in hexanes) as a yellow viscous oil. 1H NMR ($CDCl_3$, 500 MHz): δ 9.75 (s, 1H), 6.36 (br. s, 3H), 4.36 (d, $J = 15$ Hz, 2H), 3.75 (s, 6H), 3.44 (br. s, 2H), 3.16 (br. s, 4H), 2.63 (br. s, 2H), 1.67 (br. s, 2H), 1.47 (br. s, 9H), 1.40 (br. s, 9H). ^{13}C NMR ($CDCl_3$, 125 MHz): δ 201.1, 161.0, 156.0, 155.6, 105.6, 105.2, 99.1, 79.9, 55.3, 50.8, 45.9, 45.2, 44.5, 43.7, 43.4, 41.1, 28.5, 28.4. MS (ESI): m/z Calcd for $C_{25}H_{40}N_2O_7$ $[M + H]^+$: 481.29, found 481.18.

17. Following general procedure C (based on 8.0 g of **12**), 7.7 g (97%) of **17** was isolated (SiO_2 : $R_F = 0.3$, 60/40 v/v EtOAc in hexanes) as a yellow viscous oil. 1H and ^{13}C NMR spectra are provided in the SI. HR-MS (ESI): m/z Calcd for $C_{41}H_{71}N_4O_{11}$ $[M + H]^+$: 795.5114, found 795.5118; Calcd for $C_{41}H_{70}N_4NaO_{11}$ $[M + Na]^+$: 817.4933, found 817.4947.

18. Following general procedure C (based on 6.1 g of **13**), 4.7 g (69%) of **18** was isolated (SiO_2 : $R_F = 0.4$, 70/30 v/v EtOAc in hexanes) as a yellow viscous oil. 1H and ^{13}C NMR spectra are provided in the SI. HR-MS (ESI): m/z Calcd for $C_{57}H_{101}N_6O_{15}$ $[M + H]^+$: 1109.7319, found 1109.7292; Calcd for $C_{57}H_{104}N_7O_{15}$ $[M + NH_4]^+$: 1126.7585, found 1126.7589; Calcd for $C_{57}H_{100}N_6NaO_{15}$ $[M + Na]^+$: 1131.7139, found 1131.7135.

20. Following general procedure C (based on 2.8 g of **14**), 2.2 g (79%) of **20** was isolated (SiO_2 : $R_F = 0.4$, 70/30 v/v EtOAc in hexanes) as a yellow viscous oil. 1H and ^{13}C NMR spectra are provided in the SI. HR-MS (ESI): m/z Calcd for $C_{73}H_{131}N_8O_{19}$ $[M + H]^+$: 1423.9525, found 1423.9548; Calcd for $C_{73}H_{104}N_7O_{15}$ $[M + NH_4]^+$: 1126.7585, found 1126.7589; Calcd for $C_{57}H_{100}N_6NaO_{15}$ $[M + Na]^+$: 1131.7139, found 1131.7135.

General Procedure D. The requisite amine (1.0 equiv) was added to a solution of 3,5-dimethoxybenzaldehyde (**1**) (2.0 equiv) in absolute EtOH (0.2 M) and stirred for 16 h at room temperature. $NaBH_4$ (4.0 equiv) was then added in one portion and the solution was stirred for an additional 1 h before quenching the reaction with Me_2CO and concentrating in vacuo. The residue was taken up in EtOAc, washed with H_2O , dried ($MgSO_4$), and filtered through a pad of Celite, and the filtrate was concentrated in vacuo. The residue was then dissolved in concentrated HCl (12 N) and concentrated in vacuo. The residue was dissolved in H_2O and the product precipitated

by adding a saturated solution of $NH_4PF_6(aq)$. The precipitate was filtered, washed with H_2O , and air-dried, affording a white powder.

2D·2PF₆. Following general procedure D (based on 250 mg of 1,3-diaminopropane (**5**)), 2.11 g (94%) of **2D·2PF₆** was obtained as a white powder. 1H NMR (CD_3CN , 500 MHz): δ 6.61 (d, $J = 2.2$ Hz, 4H), 6.56 (t, $J = 2.2$ Hz, 2H), 4.08 (s, 4H), 3.80 (s, 12H), 3.05 (t, $J = 7.6$ Hz, 4H), 2.03 (q, $J = 7.6$ Hz, 2H). ^{13}C NMR (CD_3CN , 125 MHz): δ 161.0, 131.8, 107.5, 100.6, 54.9, 51.3, 44.1, 21.9. MS (ESI): m/z Calcd for $C_{21}H_{31}N_2O_4$ $[M - HPF_6 - PF_6]^+$: 375.23, found 375.27.

3D·3PF₆. Following general procedure D (based on 250 mg of bis(3-amino-propyl)amine (**6**)), 1.29 g (78%) of **3D·3PF₆** was obtained as a white powder. 1H NMR (CD_3CN , 500 MHz): δ 6.60 (d, $J = 2.2$ Hz, 4H), 6.58 (t, $J = 2.2$ Hz, 2H), 4.11 (t, $J = 5.4$ Hz, 4H), 3.81 (s, 12H), 3.03 (m, 8H), 2.00 (q, $J = 7.4$ Hz, 4H). ^{13}C NMR (CD_3CN , 125 MHz): δ 161.0, 131.8, 107.5, 100.7, 54.9, 51.3, 44.7, 44.1, 21.9. MS (ESI): m/z Calcd for $C_{24}H_{38}N_3O_4$ $[M - 2HPF_6 - PF_6]^+$: 432.29, found 432.30.

4D·4PF₆. Following general procedure D (based on 250 mg of N,N' -bis(3-aminopropyl)-1,3-propanediamine (**8**)), 1.00 g (70%) of **4D·4PF₆** was obtained as a white powder. 1H NMR (CD_3CN , 500 MHz): δ 6.94 (br s, 4H), 6.76 (br s, 4H), 6.61 (d, $J = 2.0$ Hz, 4H), 6.57 (t, $J = 2.0$ Hz, 2H), 4.11 (br s, 4H), 3.80 (s, 12H), 3.07 (br s, 12H), 2.03 (br s, 6H). ^{13}C NMR (CD_3CN , 125 MHz): δ 162.0, 133.04, 108.6, 101.9, 56.1, 52.5, 46.0, 45.8, 45.3, 23.1. MS (ESI): m/z Calcd for $C_{27}H_{46}F_6N_4O_4P$ $[M - 2HPF_6 - PF_6]^+$: 635.31, found 635.13; Calcd for $C_{27}H_{45}N_4O_4$ $[M - 3HPF_6 - PF_6]^+$: 489.34, found 489.36.

General Procedure E. A solution of bis(3-aminopropyl)amine (**21**) (1.0 equiv) in anhydrous EtOH (0.2 M) was added to a solution of the requisite aldehyde (2.0 equiv) in anhydrous EtOH (0.2 M) and the resulting solution was stirred at room temperature for 16 h. $NaBH_4$ (4.0 equiv) was added to the reaction mixture, which was stirred for an additional 1 h before quenching the reaction with Me_2CO and concentrating in vacuo. The residue was taken up in EtOAc, washed with H_2O , dried ($MgSO_4$), filtered through a pad of Celite, and the filtrate concentrated in vacuo. The residue was dissolved in CH_2Cl_2 /TFA (1/1, 0.1 M) and stirred for 24 h at room temperature. The solvent was removed in vacuo and the residue was dissolved in H_2O and the product precipitated by adding a saturated solution of $NH_4PF_6(aq)$. The precipitate was filtered, washed with H_2O , and air-dried, affording a white powder.

7D·7PF₆. Following general procedure E (based on 165 mg of the aldehyde **16**), 185 mg (79%) of **7D·7PF₆** was isolated as a white powder. 1H NMR (CD_3CN , 500 MHz): δ 6.89 (br. s, 4H), 6.72 (br. s, 10H), 6.60 (d, $J = 1.9$ Hz, 4H), 6.57 (t, $J = 1.9$ Hz, 2H), 4.11 (t, $J = 5.1$ Hz, 4H), 3.81 (s, 12H), 3.07 (br. s, 24H), 2.02 (br. s, 12H). ^{13}C (CD_3CN , 125 MHz): δ 162.3, 133.0, 108.7, 101.9, 56.1, 52.6, 46.0, 45.9, 45.9, 45.3, 23.2. HR-MS (ESI): m/z Calcd for $C_{36}H_{68}F_{12}N_7O_4P_2$ $[M - 4HPF_6 - PF_6]^+$: 952.4611, found 952.4580; Calcd for $C_{36}H_{69}F_{18}N_7O_4P_3$ $[M - 3HPF_6 - PF_6]^+$: 1098.4331, found 1098.4307.

11D·11PF₆. Following general procedure E (based on 740 mg of aldehyde **17**), 511 mg (44%) of **11D·11PF₆** was isolated as a white powder. 1H NMR (CD_3CN , 500 MHz): δ 6.93 (br. s, 4H), 6.74 (br. s, 18H), 6.60 (br. s, 4H), 6.57 (br. s, 2H), 4.11 (br. s, 4H), 3.80 (s, 12H), 3.07 (br. s, 40H), 2.02 (br. s, 10H). ^{13}C (CD_3CN , 125 MHz): δ 162.2, 133.0, 108.6, 101.9, 56.1, 52.5, 46.0, 45.9, 45.3, 23.1. HR-MS (ESI): m/z Calcd for $C_{48}H_{97}F_{18}N_{11}O_4P_3$ $[M - 7HPF_6 - PF_6]^+$: 1326.6645, found 1326.6637; Calcd for $C_{48}H_{98}F_{24}N_{11}O_4P_4$ $[M - 6HPF_6 - PF_6]^+$: 1472.6365;

found 1472.6367; Calcd for $C_{48}H_{99}F_{30}N_{11}O_4P_5$ [$M - 5HPF_6 - PF_6$] $^+$: 1618.6085; found 1618.6100; Calcd for $C_{48}H_{100}F_{36}N_{11}O_4P_6$ [$M - 4HPF_6 - PF_6$] $^+$: 1764.5805; found 1764.5817; Calcd for $C_{48}H_{101}F_{42}N_{11}O_4P_7$ [$M - 3HPF_6 - PF_6$] $^+$: 1910.5525; found 1910.5537.

15D·15PF₆. Following general procedure E (based on 235 mg of aldehyde **18**), 140 mg (40%) of **15D·15PF₆** was isolated as a white powder. ¹H NMR (CD₃CN, 500 MHz): δ 6.94 (br. s, 4H), 6.75 (br. s, 26H), 6.60 (br. s, 4H), 6.57 (br. s, 2H), 4.11 (br. s, 4H), 3.80 (s, 12H), 3.07 (br. s, 56H), 2.02 (br. s, 28H). ¹³C (CD₃CN, 125 MHz): δ 162.2, 133.1, 108.7, 101.9, 56.1, 52.5, 46.0, 45.9, 45.3, 23.2. HR-MS (ESI): *m/z* Calcd for $C_{60}H_{130}F_{48}N_{15}O_4P_8$ [$M - 6HPF_6 - PF_6$] $^+$: 2284.7559, found 2284.7616; Calcd for $C_{60}H_{129}F_{42}N_{15}O_4P_7$ [$M - 7HPF_6 - PF_6$] $^+$: 2284.7559, found 2284.7616; Calcd for $C_{60}H_{128}F_{36}N_{15}O_4P_6$ [$M - 8HPF_6 - PF_6$] $^+$: 1992.8119, found 1992.8147; Calcd for $C_{60}H_{127}F_{30}N_{15}O_4P_5$ [$M - 9HPF_6 - PF_6$] $^+$: 1846.8399, found 1846.8390; Calcd for $C_{60}H_{126}F_{24}N_{15}O_4P_4$ [$M - 10HPF_6 - PF_6$] $^+$: 1700.8679, found 1700.8638; Calcd for $C_{60}H_{125}F_{18}N_{15}O_4P_3$ [$M - 11HPF_6 - PF_6$] $^+$: 1554.8959, found 1554.9033.

19D·19PF₆. Following general procedure E (based on 103 mg of aldehyde **20**), 81 mg (54%) of **19D·19PF₆** was isolated as a white powder. ¹H NMR (CD₃CN, 500 MHz): δ 7.08 (br. s, 4H), 6.87 (br. s, 34H), 6.60 (br. s, 4H), 6.58 (br. s, 2H), 4.10 (br. s, 4H), 3.80 (s, 12H), 3.06 (br. s, 72H), 2.02 (t, *J* = 6.8 Hz, 36H). ¹³C (CD₃CN, 125 MHz): δ 162.2, 133.1, 108.7, 101.9, 56.1, 52.5, 45.9, 45.3, 23.2. HR-MS (ESI): *m/z* Calcd for $C_{102}H_{168}F_{48}N_{19}O_36$ [$M - 4CF_3COO$] $^{2+}$: 764.5315, found 764.4547.

28. A solution of methyl 4-cyanobenzoate (**27**) (5.00 g, 31.0 mmol) in THF (50 mL) was added over the course of 10 min to a suspension of LiAlH₄ (5.89 g, 155 mmol) in anhydrous THF (200 mL) at 0 °C. The reaction mixture was stirred for an additional 1 h before moving the flask to a 50 °C preheated oil bath and stirred for 16 h. The reaction mixture was then cooled to 0 °C and quenched by the slow addition of H₂O (5.9 mL), 15% NaOH_(aq) (5.9 mL), and H₂O (17.7 mL). The resulting precipitate was stirred for an additional 30 min, filtered through a pad of Celite, rinsed with THF, and the filtrate concentrated in vacuo. The residue was taken up in 1 M HCl (50 mL), extracted with CH₂Cl₂ (1 ×), and the aqueous layer concentrated in vacuo. Me₂CO (50 mL) was added to the crude solid and the suspension was filtered affording 4.42 g (81%) of pure **28** as a white solid. ¹H NMR (D₂O, 500 MHz): δ 7.41 (s, 4H), 4.61 (s, 2H), 4.14 (s, 2H). ¹³C NMR (D₂O, 125 MHz): δ 141.0, 131.9, 129.0, 128.0, 63.3, 42.7. MS (ESI): *m/z* Calcd for $C_8H_{12}NO$ [$M + H$] $^+$: 138.09, found 138.34.

General Procedure F. NaHCO₃ (1.5 equiv) was added to a solution of [4-(amino-methyl)phenyl]methanol hydrochloride (**28**) (1.0 equiv) and the appropriate aldehyde (1.0 equiv) in anhydrous MeOH, and the resulting solution was stirred at room temperature for 16 h. The reaction mixture was cooled to 0 °C, NaBH₄ (3.0 equiv) was added in portions, and the reaction mixture was stirred for an additional 1 h. The reaction was quenched by the addition of Me₂CO and concentrated in vacuo. The residue was taken up in EtOAc, washed with H₂O, brine, dried (MgSO₄), and concentrated in vacuo. The residue was purified by silica gel flash chromatography to provide typically a viscous oil.

30. Following general procedure F (based on 2.70 g of 4-formylbenzonitrile (**29**)), 4.10 g (79%) of **30** was isolated (SiO₂: R_F = 0.4, 5% MeOH in CH₂Cl₂) as a viscous oil. ¹H NMR (CD₂Cl₂, 500 MHz): δ 7.60 (d, *J* = 8.2 Hz, 2H), 7.46 (d, *J* = 8.2 Hz, 2H), 7.29 (s, 4H), 4.61 (s, 2H), 3.82 (s, 2H), 3.75

(s, 2H). ¹³C NMR (CD₂Cl₂, 125 MHz): δ 146.3, 140.2, 139.4, 132.2, 128.7, 128.3, 127.0, 119.0, 110.6, 64.7, 52.8, 52.5. MS (ESI): *m/z* Calcd for $C_{16}H_{17}N_2O$ [$M + H$] $^+$: 253.13, found 253.21.

31. Following general procedure B (based on 1.78 g of **30**), 2.56 g (89%) of **31** was isolated (SiO₂: R_F = 0.4, 2% MeOH in CH₂Cl₂) as a viscous oil. ¹H NMR (CD₂Cl₂, 500 MHz): δ 7.60 (d, *J* = 8.0 Hz, 2H), 7.30 (d, *J* = 8.0 Hz, 4H), 7.18 (br. s, 2H), 4.60 (s, 4H), 4.42 (br. s, 2H), 4.38 (br. s, 2H), 1.45 (br. s, 9H). ¹³C (CDCl₃, 125 MHz): δ 155.8, 155.7, 147.2, 144.1, 143.8, 140.7, 136.6, 132.3, 128.2, 127.9, 127.5, 127.1, 126.8, 118.8, 110.8, 80.5, 64.3, 49.9, 49.7, 49.0, 28.1. MS (ESI): *m/z* Calc for $C_{21}H_{25}N_2O_3$ [$M + H$] $^+$: 353.19, found 353.66.

32. A solution of **31** (2.56 g, 7.27 mmol) in THF (20 mL) was added over the course of 5 min to a suspension of LiAlH₄ (0.55 g, 14.5 mmol), in THF (60 mL) at 0 °C. The solution was gradually warmed to room temperature over the course of 30 min and stirred for an additional 24 h. The reaction mixture was quenched by cooling it to 0 °C and adding dropwise H₂O (0.56 mL), 15% NaOH_(aq) (0.56 mL), and H₂O (1.7 mL). The resulting suspension was stirred for an additional 30 min, filtered through a pad of Celite, and the filtrate was concentrated in vacuo. The residue was purified by silica gel flash chromatography affording 1.76 g (68%) of **32** as a viscous oil (SiO₂: R_F = 0.3, 94:6:0.5 CH₂Cl₂/MeOH/NH₄OH). ¹H NMR (CD₂Cl₂, 500 MHz): δ 7.26 (d, *J* = 8.0 Hz, 2H), 7.21 (d, *J* = 8.0 Hz, 2H), 7.14 (br. s, 4H), 4.59 (s, 2H), 4.35 (br. s, 2H), 4.31 (br. s, 2H), 3.77 (s, 2H), 1.46 (s, 9H). ¹³C (CD₂Cl₂, 125 MHz): δ 155.9, 142.1, 140.6, 137.3, 136.7, 127.9, 127.7, 127.6, 127.3, 127.1, 79.9, 64.5, 49.4, 48.9, 45.9, 28.2. MS (ESI) *m/z* Calcd for $C_{21}H_{29}N_2O_3$ [$M + H$] $^+$: 357.22, found 357.31.

34. Following general procedure F (based on 3.30 g of methyl 4-formylbenzoate (**33**)), 4.13 g (72%) of **34** was isolated (SiO₂: R_F = 0.3, 95:5:0.5 CH₂Cl₂:MeOH:NH₄OH) as a viscous oil. ¹H NMR (CDCl₃, 500 MHz): δ 7.98 (d, *J* = 8.3 Hz, 2H), 7.39 (d, *J* = 8.0 Hz, 2H), 7.30 (br. s, 2H), 4.64 (s, 2H), 3.90 (s, 3H), 3.82 (s, 2H), 3.77 (s, 3H). ¹³C (CDCl₃, 125 MHz): δ 167.2, 145.6, 140.0, 139.3, 129.8, 128.9, 128.4, 128.1, 127.2, 65.0, 52.9, 52.7, 52.2. MS (ESI): *m/z* Calcd for $C_{17}H_{20}NO_3$ [$M + H$] $^+$: 286.14, found 286.24.

35. Following general procedure B (based on 3.99 g of **34**), 5.22 g of **35** (97%) was isolated (R_F = 0.4, 2% MeOH in CH₂Cl₂) as a viscous oil. ¹H NMR (CD₂Cl₂, 500 MHz): δ 7.95 (d, *J* = 8.2 Hz, 2H), 7.29 (d, *J* = 8.2 Hz, 2H), 7.25 (br. s, 2H), 7.17 (br. s, 2H), 4.63 (d, *J* = 5.4 Hz, 2H), 4.41 (br. s, 2H), 4.36 (br. s, 2H), 3.86 (s, 3H), 1.96 (t, *J* = 5.4 Hz, 1H), 1.44 (br. s, 9H). ¹³C (CD₂Cl₂, 125 MHz): δ 166.8, 155.8, 143.9, 143.7, 140.4, 137.2, 129.7, 129.2, 128.0, 127.6, 127.2, 80.2, 64.8, 52.0, 49.6, 49.0, 28.1. MS (ESI): *m/z* Calcd for $C_{22}H_{28}NO_5$ [$M + H$] $^+$: 386.20, found 386.40.

36. A solution of **35** (4.67 g, 12.1 mmol) in anhydrous THF (40 mL) was added over the course of 10 min to a 1.0 M solution of DIBAL in THF (48.5 mL, 48.5 mmol) at 0 °C. The reaction mixture was gradually warmed to room temperature and stirred for a total of 5 h before cooling back down to 0 °C and quenching by the slow addition of H₂O (1.9 mL), 15% NaOH_(aq) (1.9 mL), and H₂O (4.9 mL). The resulting solution was stirred for a further 30 min and then filtered through a pad of Celite. The filtrate was concentrated in vacuo and the residue was purified by silica gel flash chromatography to afford 3.05 g (70%) of **36** as a viscous oil (SiO₂: R_F = 0.4, 4% MeOH in CH₂Cl₂). ¹H NMR (CD₂Cl₂, 500 MHz): δ 7.27 (d, *J* = 8.2 Hz, 4H), 7.16 (br. s, 4H), 4.61 (d, *J* = 5.5 Hz, 4H), 4.35 (br. s, 2H),

4.31 (br. s, 2H), 2.15 (t, $J = 5.5$ Hz, 2H), 1.46 (s, 9H). ^{13}C (CD_2Cl_2 , 125 MHz): δ 155.9, 140.3, 137.4, 128.0, 127.7, 80.0, 64.8, 49.4, 48.9, 28.2. MS (ESI): m/z Calcd for $\text{C}_{21}\text{H}_{28}\text{NO}_4$ [$M + \text{H}$] $^+$: 358.20, found 358.29.

37. Following general procedure C (based on 2.00 g of **36**), 1.78 g (88%) of **37** was isolated as a viscous oil (SiO_2 : $R_F = 0.4$, 60/40 v/v EtOAc in hexanes). ^1H NMR (CDCl_3 , 500 MHz): δ 9.99 (s, 2H), 7.84 (d, $J = 8.1$ Hz, 4H), 7.35 (br. d, 4H), 4.53 (br. s, 2H), 4.42 (br. s, 2H), 1.46 (s, 9H). ^{13}C (CDCl_3 , 125 MHz): δ 207.2, 191.9, 155.8, 145.0, 144.8, 135.8, 130.2, 128.4, 127.7, 81.0, 50.1, 49.8, 31.0, 28.4. MS (ESI): m/z Calcd for $\text{C}_{21}\text{H}_{24}\text{NO}_4$ [$M + \text{H}$] $^+$: 354.17, found 354.23.

General Procedure G. A solution of amine **32** (2.0 equiv) in anhydrous EtOH (0.2 M) was added to a solution of the requisite dialdehyde (1.0 equiv) in anhydrous EtOH (0.2 M) and the resulting reaction mixture was stirred at room temperature for 16 h. NaBH_4 (2.0 equiv) was added to the reaction mixture, which was stirred for an additional 5 h before being concentrated in vacuo. The residue was dissolved in EtOAc, washed with H_2O , dried (MgSO_4), and filtered through a pad of Celite, and the filtrate was concentrated in vacuo to provide the diol-terminated dumbbell which was purified by silica gel flash chromatography to provide typically a viscous oil.

38. Following general procedure G (based on 2.80 g of **37**), 3.45 g (85%) of **38** was isolated (SiO_2 : $R_F = 0.3$, 95:5:0.5 $\text{CH}_2\text{Cl}_2/\text{MeOH}/\text{NH}_4\text{OH}$) as a viscous oil. ^1H NMR (CD_2Cl_2 , 500 MHz): δ 7.29–7.25 (m, 12H), 7.15 (br. s, 12H), 4.59 (s, 4H), 4.36 (br. s, 6H), 4.31 (br. s, 6H), 3.76 (s, 4H), 3.74 (s, 4H), 1.45 (s, 27H). ^{13}C (CD_2Cl_2 , 125 MHz): δ 155.8, 140.3, 139.4, 137.6, 136.9, 128.3, 127.9, 127.6, 127.1, 79.9, 79.8, 64.8, 52.8, 49.4, 49.0, 28.2. MS (ESI): m/z Calcd for $\text{C}_{63}\text{H}_{80}\text{N}_5\text{O}_8$ [$M + \text{H}$] $^+$: 1034.60, found 1034.12.

40. Following general procedure B (based on 3.32 g of **38**), 3.03 g (77%) of **40** was isolated (SiO_2 : $R_F = 0.4$, 4% MeOH in CH_2Cl_2) as a colorless oil. ^1H NMR (CD_2Cl_2 , 500 MHz): δ 7.29 (d, $J = 8.2$ Hz, 4H), 7.16 (br. s, 20 H), 4.63 (d, $J = 5.4$ Hz, 4H), 4.36 (br. s, 10H), 4.31 (br. s, 10H), 1.46 (s, 45H). ^{13}C (CD_2Cl_2 , 125 MHz): δ 155.8, 140.3, 139.4, 137.6, 136.9, 128.3, 127.9, 127.6, 127.1, 79.9, 79.8, 64.8, 52.8, 49.4, 49.9, 28.2. MS (ESI): m/z Calcd for $\text{C}_{73}\text{H}_{96}\text{N}_5\text{O}_{12}$ [$M + \text{H}$] $^+$: 1234.71, found 1234.55.

42. Following general procedure C (based on 240 mg of **40**), 177 mg (74%) of **42** was isolated (SiO_2 : $R_F = 0.2$ 60/40 \rightarrow 75/25 v/v EtOAc in hexanes) as a colorless oil. ^1H NMR (CD_2Cl_2 , 500 MHz): δ 9.96 (s, 2H), 7.81 (d, $J = 8.2$ Hz, 4H), 7.35 (br. s, 4H), 7.18 (br. s, 16H), 4.43–4.32 (m, 20H), 1.46 (s, 45H). ^{13}C (CD_2Cl_2 , 500 MHz): δ 191.8, 155.8, 137.4, 137.3, 136.6, 129.9, 128.0, 127.8, 80.3, 79.9, 49.8, 49.6, 49.2, 48.7, 28.2. MS (ESI): m/z Calcd for $\text{C}_{125}\text{H}_{160}\text{N}_9\text{O}_{20}$ [$M + \text{H}$] $^+$: 1054.09, found 1054.43.

39. Following general procedure G (based on 561 mg of **42**), 735 mg (84%) of **39** was isolated (SiO_2 : $R_F = 0.4$, 95:5:0.5 $\text{CH}_2\text{Cl}_2/\text{MeOH}/\text{NH}_4\text{OH}$) as a viscous oil. ^1H NMR (CDCl_3 , 500 MHz): δ 7.29 (m, 12H), 7.19 (m, 28H), 4.66 (s, 4H), 4.40 (s, 14H), 4.32 (s, 14H), 3.81 (s, 4H), 3.79 (s, 4H), 1.50 (s, 63H). ^{13}C (CDCl_3 , 125 MHz): 156.1, 140.1, 139.1, 137.5, 137.1, 136.9, 128.5, 128.4, 128.3, 127.8, 127.4, 80.3, 80.2, 65.2, 53.6, 53.0, 49.3, 49.1, 48.7, 28.6. MS (ESI): m/z Calcd for $\text{C}_{115}\text{H}_{148}\text{N}_9\text{O}_{16}$ [$M + \text{H}$] $^+$: 1911.10, found 1911.22.

41. Following general procedure B (based on 725 mg of **39**), 705 mg (88%) of **41** was isolated (SiO_2 : $R_F = 0.4$, 3% MeOH in CH_2Cl_2) as a colorless oil. ^1H NMR (CD_2Cl_2 , 500 MHz): δ 7.33 (d, $J = 6.9$ Hz, 4H), 7.24 (br. s, 36H), 4.63 (s, 4H), 4.43

(br. s, 18H), 4.38 (br. s, 18H), 1.52 (br. s, 81H). ^{13}C (CD_2Cl_2 , 125 MHz): δ 155.9, 146.8, 140.8, 137.2, 128.0, 127.8, 127.0, 85.2, 78.0, 79.9, 64.4, 49.3, 48.8, 28.3, 27.2. MS (ESI): m/z Calcd for $\text{C}_{125}\text{H}_{165}\text{N}_9\text{O}_{20}$ [$M + 2\text{H}$] $^{2+}$: 1056.11, found 1056.34.

43. Following general procedure C (based on 310 mg of **41**), 264 mg (85%) of **43** was isolated (SiO_2 : $R_F = 0.3$, 60/40 v/v EtOAc in hexanes) as a colorless oil. ^1H NMR (CD_2Cl_2 , 500 MHz): δ 9.96 (s, 2H), 7.81 (d, $J = 8.5$ Hz, 4H), 7.35 (br. s, 4H), 7.18 (br. s, 32H), 4.37 (br. s, 18H), 4.32 (br. s, 18H), 1.46 (br. s, 81H). ^{13}C (CD_2Cl_2 , 125 MHz): δ 206.5, 191.8, 191.8, 155.8, 137.4, 137.3, 136.9, 135.6, 129.9, 127.9, 127.8, 80.2, 79.9, 80.2, 79.9, 49.8, 49.2, 48.7, 30.7, 28.2. MS (ESI): m/z Calcd for $\text{C}_{125}\text{H}_{160}\text{N}_9\text{O}_{20}$ [$M + 2\text{H}$] $^{2+}$: 1054.09, found 1054.71.

General Procedure H. A solution of 3,5-dimethoxybenzylamine (**23**) (2.0 equiv) in anhydrous EtOH (0.2 M) was added to a solution of the requisite dialdehyde (1.0 equiv) in anhydrous EtOH (0.2 M) and the resulting solution was stirred at room temperature for 16 h. NaBH_4 (2.0 equiv) was added to the reaction mixture, which was stirred for an additional 5 h before being concentrated in vacuo. The residue was taken up in EtOAc, washed with H_2O , dried (MgSO_4), filtered through a pad of Celite, and concentrated in vacuo. The residue was dissolved in $\text{CH}_2\text{Cl}_2/\text{TFA}$ (1/1, 0.1 M) and allowed to stir for 24 h at room temperature. The solvent was removed in vacuo, dissolved in an equal volume of H_2O , and precipitated by adding a saturated solution of $\text{NH}_4\text{PF}_6(\text{aq})$. The precipitate was filtered, rinsed with H_2O , and air-dried, affording a white powder.

2D'-2PF₆. Following general procedure D (based on 100 mg of *p*-xylylenediamine), 481 mg (90%) of **2D'-2PF₆** was isolated as a white powder. ^1H NMR (CD_3CN , 500 MHz): δ 7.53 (s, 4H), 7.19 (br. s, 4H), 6.61 (d, $J = 2.2$ Hz, 4H), 6.56 (t, $J = 2.2$ Hz, 2H), 4.24 (br. s, 4H), 4.16 (br. s, 4H), 3.79 (s, 12H). ^{13}C (CD_3CN , 125 MHz): δ 162.2, 133.1, 132.8, 131.7, 108.8, 101.9, 56.1, 52.4, 51.6. HR-MS (ESI): m/z Calcd for $\text{C}_{26}\text{H}_{34}\text{F}_6\text{N}_2\text{O}_4\text{P}$ [$M - \text{PF}_6$] $^+$: 583.2155, found 583.2156; Calcd for $\text{C}_{26}\text{H}_{33}\text{N}_2\text{O}_4$ [$M - \text{HPF}_6 - \text{PF}_6$] $^+$: 437.2435; found 437.2449.

3D'-3PF₆. Following general procedure H (based on 153 mg of **24**), 245 mg (97%) of **3D'-3PF₆** was isolated as a white powder. ^1H NMR ($\text{Me}_2\text{SO}-d_6$, 500 MHz): δ 9.27 (br. s, 6H), 7.55 (s, 8H), 6.66 (d, $J = 2.2$ Hz, 4H), 6.57 (t, $J = 2.2$ Hz, 2H), 4.20 (br. s, 8H), 4.18 (br. s, 4H), 4.10 (s, 12H). ^{13}C ($\text{Me}_2\text{SO}-d_6$, MHz): δ 160.7, 133.7, 132.5, 130.3, 107.8, 100.5, 55.4, 50.1, 49.8, 49.6. HR-MS (ESI): m/z Calcd for $\text{C}_{34}\text{H}_{44}\text{F}_{12}\text{N}_3\text{O}_4\text{P}_2$ [$M - \text{PF}_6$] $^+$: 848.2610, found 848.2623; Calcd for $\text{C}_{34}\text{H}_{43}\text{F}_{12}\text{N}_3\text{O}_4\text{P}$ [$M - \text{HPF}_6 - \text{PF}_6$] $^+$: 702.2890, found 702.2947; Calcd for $\text{C}_{34}\text{H}_{42}\text{N}_3\text{O}_4$ [$M - 2\text{HPF}_6 - \text{PF}_6$] $^+$: 556.3170, found 556.3302.

7D'-7PF₆. Following general procedure H (based on 98 mg of **25**), 136 mg (83%) of **7D'-7PF₆** was isolated as a white solid. ^1H NMR (CD_3CN , 500 MHz): δ 9.03 (br. s, 14H), 7.52 (s, 24H), 6.62 (d, $J = 2.2$ Hz, 4H), 6.53 (t, $J = 2.2$ Hz, 2H), 4.13 (br. s, 24H), 4.03 (br. s, 4H), 3.77 (s, 12H). ^{13}C (CD_3CN , 125 MHz): δ 162.0, 131.4, 131.3, 108.7, 101.3, 56.1, 51.5, 51.3, 50.9. HR-MS (ESI): m/z Calcd for $\text{C}_{66}\text{H}_{83}\text{F}_{30}\text{N}_7\text{O}_4\text{P}_5$ [$M - \text{HPF}_6 - \text{PF}_6$] $^+$: 1762.4710, found 1762.4762; Calcd for $\text{C}_{66}\text{H}_{81}\text{F}_{18}\text{N}_7\text{O}_4\text{P}_3$ [$M - 3\text{HPF}_6 - \text{PF}_6$] $^+$: 1470.5270, found 1470.5250; Calcd for $\text{C}_{66}\text{H}_{80}\text{F}_{12}\text{N}_7\text{O}_4\text{P}_2$ [$M - 4\text{HPF}_6 - \text{PF}_6$] $^+$: 1324.5550, found 1324.5520, Calcd for $\text{C}_{66}\text{H}_{79}\text{F}_6\text{N}_7\text{O}_4\text{P}$ [$M - 5\text{HPF}_6 - \text{PF}_6$] $^+$: 1178.5830, found 1178.5791, Calcd for $\text{C}_{66}\text{H}_{78}\text{N}_7\text{O}_4$ [$M - 6\text{HPF}_6 - \text{PF}_6$] $^+$: 1032.6110, found 1032.6085, Calcd for $\text{C}_{66}\text{H}_{84}\text{F}_{30}\text{N}_7\text{O}_4\text{P}_5$ [$M - 2\text{PF}_6$] $^{2+}$: 881.7392, found 881.7430.

11D'·11PF₆. Following general procedure H (based on 42 mg of **26**), 53 mg (53%) of **11D'·11PF₆** was isolated as a white powder. ¹H NMR (CD₃CN, 500 MHz): δ 9.89 (br. s, 22H), 7.51 (s, 40H), 6.64 (d, *J* = 2.2 Hz, 4H), 6.49 (t, *J* = 2.2 Hz, 2H), 4.15 (br. s, 34H), 4.12 (br. s, 4H), 4.05 (br. s, 4H), 3.74 (s, 12H). ¹³C (CD₃CN, 125 MHz): δ 162.2, 133.3, 131.8, 108.7, 101.9, 56.1, 52.2. HR-MS (ESI): *m/z* Calcd for C₉₈H₁₁₈F₂₄N₁₁O₄P₄ [M - 6HPF₆-PF₆]⁺: 2092.7930, found 2092.7862, Calcd for C₉₈H₁₁₆F₁₂N₁₁O₄P₂ [M - 8HPF₆-PF₆]⁺: 1800.8490, found 1800.8455, Calcd for C₉₈H₁₁₅F₆N₁₁O₄P [M - 9HPF₆-PF₆]⁺: 1654.8770, found 1654.8726; Calcd for C₉₈H₁₁₄N₁₁O₄[M - 10HPF₆-PF₆]⁺: 1508.9050, found 1508.9052.

General Procedure I. In a typical procedure, the appropriate oligo-ammonium dumbbell (1.0 equiv) was added to a solution of 2,6-pyridinedicarboxaldehyde (**44**) (*n* equiv, *n* = number of ammonium recognition sites), and tetraethyleneglycol bis(2-amino-phenyl)ether (**45**) (*n* equiv) in MeCN (0.5 M) and stirred until equilibrium is reached (Table 1). Neat *i*Pr₂O was layered on top of the MeCN solution until precipitation of the oligorotaxane was complete. The precipitate was collected by filtration, washed with *i*Pr₂O, and air-dried to afford the oligorotaxane as a typically bright yellow powder.

2R·2PF₆. Following general procedure I (based on 33 mg of **2D·2PF₆**), 78 mg (93%) of **2R·2PF₆** was isolated as a yellow powder. ¹H NMR (CD₃CN, 500 MHz): δ 9.40 (br. s, 4H), 8.30 (s, 4H), 7.75 (t, *J* = 7.8 Hz, 2H), 7.59 (d, *J* = 7.8 Hz, 4H), 7.20 (t, *J* = 8.0 Hz, 4H), 6.99 (d, *J* = 2 Hz, 4H), 6.72 (t, *J* = 8.0 Hz, 4H), 6.70 (d, *J* = 8.0 Hz, 4H), 6.19 (d, *J* = 2.2 Hz, 4H), 5.97 (t, *J* = 2.2 Hz, 2H), 4.37 (t, *J* = 6.8 Hz, 4H), 4.24–4.21 (m, 8H), 3.82–3.78 (m, 4H), 3.74–3.70 (m, 4H), 3.58–3.37 (m, 20H), 3.25 (s, 12H), 1.9 (br. s, 2H). ¹³C NMR (CD₃CN, 125 MHz): δ 161.3, 160.0, 151.3, 151.1, 139.6, 138.8, 134.2, 129.6, 128.4, 121.0, 120.4, 112.1, 106.4, 100.2, 69.7, 69.6, 68.4, 67.8, 54.2, 50.8, 44.7, 23.1. HR-MS (ESI): *m/z* Calcd for C₇₅H₉₀F₆N₈O₁₄P [M - PF₆]⁺: 1471.6217, found 1471.6220. Good quality single crystals suitable for X-ray diffraction analysis were grown by liquid–liquid diffusion of *i*Pr₂O into a solution of **2R·2PF₆** in CH₂Cl₂.

3R·3PF₆. Following general procedure I (based on 43 mg of **3D·3PF₆**), 103 mg (90%) of **3R·3PF₆** was isolated as a yellow powder. ¹H NMR (CD₃CN, 500 MHz): δ 9.29 (br. s, 4H), 8.99 (br. s, 2H), 8.23 (s, 4H), 8.14 (s, 2H), 7.72 (t, *J* = 7.7 Hz, 2H), 7.54 (d, *J* = 7.7 Hz, 4H), 7.47 (d, *J* = 7.7 Hz, 2H), 7.36 (t, *J* = 7.7 Hz, 1H), 7.14–7.08 (m, 6H), 6.92 (d, *J* = 8.3 Hz, 4H), 6.78 (d, *J* = 8.3 Hz, 2H), 6.61 (d, *J* = 8.3 Hz, 4H), 6.56 (t, *J* = 8.3 Hz, 4H), 6.48 (d, *J* = 8.3 Hz, 2H), 6.39 (t, *J* = 8.3 Hz, 2H), 6.15 (d, *J* = 2.3 Hz, 4H), 5.94 (t, *J* = 2.3 Hz, 2H), 4.22 (t, *J* = 7.0 Hz, 4H), 4.15–4.13 (m, 8H), 3.89 (t, *J* = 3.9 Hz, 4H), 3.76–3.32 (m, 36H), 3.33 (br. s, 4H), 3.18 (br. s, 4H), 3.26 (s, 12H), 1.72 (br. s, 4H). ¹³C NMR: see SI. HR-MS (ESI): *m/z* Calcd for C₁₀₅H₁₂₇F₁₂N₁₂O₁₉P₂ [M - PF₆]⁺: 2149.8622, found 2149.8608; Calcd for C₁₀₅H₁₂₇F₆N₁₂O₁₉P₁ [M - 2PF₆]²⁺: 1002.4490, found 1002.4507; Calcd for C₁₀₅H₁₂₇N₁₂O₁₉ [M - 3PF₆]³⁺: 619.9780, found 619.9806. X-ray quality single crystals were grown by the vapor diffusion of *tert*-butylmethylether into a solution of **3R·3PF₆** in MeOH.

4R·4PF₆. Following general procedure I (based on 53 mg of **4D·4PF₆**), 110 mg (88%) of **4R·4PF₆** was isolated as a yellow powder. ¹H NMR (CD₃CN, 500 MHz): δ 9.25 (br. s, 4H), 8.90 (br. s, 4H), 8.20 (s, 4H), 8.07 (s, 4H), 7.69 (t, *J* = 7.7 Hz, 2H), 7.52 (d, *J* = 7.7 Hz, 4H), 7.42 (d, *J* = 7.7 Hz, 4H), 7.32 (t, *J* = 7.7 Hz, 2H), 7.10 (t, *J* = 8.4 Hz, 4H), 7.04 (t, *J* = 8.4 Hz, 4H), 6.92 (d, *J* = 8.4 Hz, 4H), 6.70 (d, *J* = 8.4 Hz, 4H), 6.56 (d, *J* =

7.3 Hz, 4H), 6.51 (t, *J* = 7.3 Hz, 4H), 6.36 (t, *J* = 7.3 Hz, 4H), 6.29 (t, *J* = 7.3 Hz, 4H), 6.12 (d, *J* = 1.9 Hz, 4H), 5.91 (t, *J* = 1.9 Hz, 2H), 4.18–4.08 (m, 12H), 3.81–3.72 (m, 8H), 3.67 (br. s, 8H), 3.55–3.52 (m, 15H), 3.42–3.32 (m, 30H), 3.27 (s, 12H), 3.10–3.05 (m, 7H), 1.65 (br. s, 4H), 1.47 (br. s, 2H). ¹³C NMR: see SI. HR-MS (ESI): *m/z* Calcd for C₁₃₅H₁₆₄F₁₂N₁₆O₂₄P₂ [M - 2PF₆]²⁺: 1341.5689, found 1341.5625; Calcd for C₁₃₅H₁₆₄F₆N₁₆O₂₄P₁ [M - 3PF₆]³⁺: 846.0577, found 846.0558.

7R·7PF₆. Following general procedure I (based on 25 mg of **7D·7PF₆**), 79 mg (94%) of **7R·7PF₆** was isolated as a yellow powder. ¹H and ¹³C NMR spectra are provided in the SI. HR-MS (ESI): *m/z* Calcd for C₂₂₅H₂₇₅F₂₄N₂₈O₃₉P₄ [M - 3PF₆]³⁺: 1524.2982, found 1524.2985; Calcd for C₂₂₅H₂₇₅F₁₈N₂₈O₃₉P₃ [M - 4PF₆]⁴⁺: 1106.9825, found 1106.9836; Calcd for C₂₂₅H₂₇₅F₁₂N₂₈O₃₉P₂ [M - 5PF₆]⁵⁺: 856.5930, found 856.5903.

11R·11PF₆. Following general procedure I (based on 15 mg of **11D·11PF₆**), 45 mg (98%) of **11R·11PF₆** was isolated as a yellow powder. ¹H and ¹³C NMR spectra are provided in the SI. HR-MS (ESI): *m/z* Calcd for C₂₄₅H₄₂₃F₄₂N₄₄O₅₉P₇ [M - 4PF₆]⁴⁺: 1786.2642, found 1786.2763; Calcd for C₂₄₅H₄₂₃F₃₆N₄₄O₅₉P₆ [M - 5PF₆]⁵⁺: 1400.0184, found 1400.0153; Calcd for C₂₄₅H₄₂₃F₃₀N₄₄O₅₉P₅ [M - 6PF₆]⁶⁺: 1142.5212, found 1142.5061; Calcd for C₂₄₅H₄₂₃F₂₄N₄₄O₅₉P₄ [M - 7PF₆]⁷⁺: 958.5946, found 958.5858.

15R·15PF₆. Following general procedure I (based on 15 mg of **15D·15PF₆**), 44 mg (93%) of **15R·15PF₆** was isolated as a yellow powder. ¹H and ¹³C NMR spectra are provided in the SI. HR-MS (ESI): *m/z* Calcd for C₄₆₅H₅₇₁F₆₀N₆₀O₇₉P₁₀ [M - 5PF₆]⁵⁺: 1942.9006, found 1942.8957; Calcd for C₄₆₅H₅₇₁F₅₄N₆₀O₇₉P₉ [M - 6PF₆]⁶⁺: 1594.9230, found 1595.9068; Calcd for C₄₆₅H₅₇₁F₄₈N₆₀O₇₉P₈ [M - 7PF₆]⁷⁺: 1346.3676, found 1346.3478; Calcd for C₄₆₅H₅₇₁F₃₆N₆₀O₇₉P₆ [M - 9PF₆]⁹⁺: 1014.9604, found 1014.9535; Calcd for C₄₆₅H₅₇₁F₃₀N₆₀O₇₉P₅ [M - 10PF₆]¹⁰⁺: 898.9679, found 898.9877.

19R·19PF₆. Following general procedure I (based on 15 mg of **19D·19PF₆**), 43 mg (90%) of **19R·19PF₆** was isolated as a yellow powder. ¹H and ¹³C NMR spectra are provided in the SI. HR-MS (ESI): *m/z* Calcd for C₅₈₅H₇₁₉F₇₂N₇₆O₉₉P₁₂ [M - 7PF₆]⁷⁺: 1734.1406, found 1734.1194; Calcd for C₅₈₅H₇₁₉F₆₆N₇₆O₉₉P₁₁ [M - 8PF₆]⁸⁺: 1499.2524, found 1499.1830; Calcd for C₅₈₅H₇₁₉F₆₀N₇₆O₉₉P₁₀ [M - 9PF₆]⁹⁺: 1316.5617, found 1316.6811, Calcd for C₅₈₅H₇₁₉F₅₄N₇₆O₉₉P₉ [M - 10PF₆]¹⁰⁺: 1170.4090, found 1170.5047, Calcd for C₅₈₅H₇₁₉F₄₈N₇₆O₉₉P₈ [M - 11PF₆]¹¹⁺: 1050.8296, found 1050.6512.

2R'·2PF₆. Following general procedure I (based on 25 mg of **2D'·2PF₆**), 50 mg (86%) of **2R'·2PF₆** was isolated as a yellow powder. ¹H NMR (CD₃CN, 500 MHz): δ 9.75 (br. s, 4H), 8.28 (s, 4H), 7.90 (t, *J* = 7.6 Hz, 2H), 7.54 (d, *J* = 7.6 Hz, 4H), 7.31 (t, *J* = 8.6 Hz, 4H), 7.11 (d, *J* = 7.6 Hz, 4H), 6.92 (t, *J* = 7.6 Hz, 4H), 6.71 (d, *J* = 7.6 Hz, 4H), 6.67 (s, 4H), 6.35 (d, *J* = 2.2 Hz, 4H), 5.97 (t, *J* = 2.2 Hz, 2H), 4.55 (t, *J* = 6.8 Hz, 4H), 4.40 – 4.37 (m, 8H), 4.27 (t, *J* = 6.8 Hz, 4H), 3.91 – 3.88 (m, 4H), 3.82 – 3.79 (m, 4H), 3.53 – 3.52 (m, 8H), 3.46 – 3.45 (m, 8H), 3.34 (s, 12H). ¹³C (CD₃CN, 500 MHz): δ 162.1, 161.1, 152.7, 152.6, 141.1, 139.7, 135.3, 133.5, 130.2, 130.0, 129.6, 122.4, 121.7, 113.3, 108.3, 101.3, 71.4, 71.2, 70.1, 69.5, 55.5, 52.8, 52.1. HR-MS (ESI): *m/z* Calcd for C₈₀H₉₂F₆N₈O₁₄P [M - PF₆]⁺: 1533.6369, found 1533.6300; Calcd for C₈₀H₉₁N₈O₁₄ [M - HPF₆-PF₆]⁺: 1387.6649, found 1387.6610; Calcd for C₈₀H₉₂N₈O₁₄ [M - 2PF₆]²⁺: 694.3361, found 694.3370.

3R'·3PF₆. Following general procedure I (based on 25 mg of **3D'·3PF₆**), 44 mg (72%) of **3R'·3PF₆** was isolated as a yellow

powder. ^1H NMR (CD_3CN , 500 MHz): δ 9.72 (br. s, 4H), 9.55 (br. s, 2H), 8.27 (s, 4H), 8.10 (s, 2H), 7.90 (t, $J = 7.6$ Hz, 2H), 7.74 (t, $J = 7.6$ Hz, 1H), 7.55 (d, $J = 7.6$ Hz, 4H), 7.36 (d, $J = 7.6$ Hz, 2H), 7.31–7.26 (m, 6H), 7.10 (d, $J = 8.2$ Hz, 4H), 7.04 (d, $J = 8.2$ Hz, 2H), 6.90 (t, $J = 8.2$ Hz, 4H), 6.83 (t, $J = 8.2$ Hz, 2H), 6.70 (d, $J = 8.2$ Hz, 4H), 6.65 (d, $J = 8.2$ Hz, 4H), 6.60 (d, $J = 8.2$ Hz, 4H), 6.57 (d, $J = 8.2$ Hz, 2H), 6.35 (d, $J = 2.2$ Hz, 4H), 5.96 (t, $J = 2.2$ Hz, 2H), 4.54 (t, $J = 6.4$ Hz, 4H), 4.39–4.20 (m, 16H), 3.92–3.71 (m, 16H), 3.54–3.37 (m, 24H), 3.34 (s, 12H). ^{13}C NMR spectrum is provided in the SI. HR-MS (ESI): m/z Calcd for $\text{C}_{115}\text{H}_{130}\text{F}_6\text{N}_{12}\text{O}_{19}\text{P}$ [$M - \text{HPF}_6 - \text{PF}_6$] $^+$: 2127.9212, found 2127.9460; Calcd for $\text{C}_{115}\text{H}_{131}\text{F}_6\text{N}_{12}\text{O}_{19}\text{P}$ [$M - 2\text{PF}_6$] $^{2+}$: 1064.4642, found 1064.4621; Calcd for $\text{C}_{115}\text{H}_{130}\text{N}_{12}\text{O}_{19}$ [$M - 3\text{PF}_6$] $^{3+}$: 661.3212, found 661.3218.

7R'·7PF₆. Following general procedure I (based on 20 mg of **7D'·7PF₆**), 41 mg (78%) of **7R'·7PF₆** was isolated as a yellow powder. ^1H and ^{13}C NMR spectra are provided in the SI. HR-MS (ESI): m/z Calcd for $\text{C}_{255}\text{H}_{287}\text{F}_{24}\text{N}_{28}\text{O}_{39}\text{P}_4$ [$M - 3\text{PF}_6$] $^{3+}$: 1648.3285, found 1648.3337; Calcd for $\text{C}_{255}\text{H}_{287}\text{F}_{18}\text{N}_{28}\text{O}_{39}\text{P}_3$ [$M - 4\text{PF}_6$] $^{4+}$: 1200.0060, found 1200.0076; Calcd for $\text{C}_{255}\text{H}_{287}\text{F}_{12}\text{N}_{28}\text{O}_{39}\text{P}_2$ [$M - 5\text{PF}_6$] $^{5+}$: 931.0118, found 931.0120; Calcd for $\text{C}_{255}\text{H}_{287}\text{F}_6\text{N}_{28}\text{O}_{39}\text{P}$ [$M - 6\text{PF}_6$] $^{6+}$: 751.6824, found 751.6797.

11R'·11PF₆. Following general procedure I (based on 15 mg of **11D'·11PF₆**), 32 mg (85%) of **11R'·11PF₆** was isolated as a yellow powder. ^1H and ^{13}C NMR spectra are provided in the SI. HR-MS (ESI): m/z Calcd for $\text{C}_{345}\text{H}_{423}\text{F}_{48}\text{N}_{44}\text{O}_{59}\text{P}_8$ [$M - 3\text{PF}_6$] $^{3+}$: 2428.6190, found 2428.6179; Calcd for $\text{C}_{345}\text{H}_{423}\text{F}_{42}\text{N}_{44}\text{O}_{59}\text{P}_7$ [$M - 4\text{PF}_6$] $^{4+}$: 1785.2231, found 1785.3202.

■ ASSOCIATED CONTENT

● Supporting Information

Detailed X-ray crystallographic analysis data and ^1H and ^{13}C NMR spectra. This material is available free of charge via the Internet at <http://pubs.acs.org>.

■ AUTHOR INFORMATION

Corresponding Author

stoddart@northwestern.edu; l.cronin@chem.gla.ac.uk

Notes

The authors declare no competing financial interest.

■ ACKNOWLEDGMENTS

We (M.E.B., C.V., R.A.S., D.C.F., and J.F.S.) at Northwestern University acknowledge support from the Air Force Office of Scientific Research (AFSOR) under the Multidisciplinary Research Program of the University Research Initiative (MURI) Award FA9550-07-1-0534 on "Bioinspired Supramolecular Enzymatic Systems" and the National Science Foundation (NSF) under the auspices of Award CHE-0924620. We also acknowledge support by the Microelectronics Advanced Research Corporation (MARCO) and its Focus Centre Research Program (FCRP) on Functional Engineered NanoArchitectonics (FENA) as well as support from the Non-Equilibrium Energy Research Centre (NERC), which is an Energy Frontier Research Centre (EFRC) funded by the U.S. Department of Energy, Office of Basic Sciences (DOE-BES) under Award DE-SC0000989. J.F.S. was supported by the WCU Program (NRF R-31-2008-000-10055-0) funded by the Ministry of Education, Science and Technology, Korea. The IM-MS work was supported by the University of Glasgow and the EPSRC. L.C. thanks the Royal Society/Wolfson Foundation for a merit award.

■ REFERENCES

- (1) (a) Stoddart, J. F.; Colquhoun, H. M. *Tetrahedron* **2008**, *64*, 8231–8263. (b) Stoddart, J. F. *Chem. Soc. Rev.* **2009**, *38*, 1802–1820. (c) Beves, J. E.; Blight, B. A.; Campbell, C. J.; Leigh, D. A.; McBurney, R. T. *Angew. Chem., Int. Ed.* **2011**, *50*, 9260–9327.
- (2) Wasserman, E. *J. Am. Chem. Soc.* **1960**, *82*, 4433–4434.
- (3) (a) Frisch, H. L.; Wasserman, E. *J. Am. Chem. Soc.* **1961**, *83*, 3789–3795. (b) Harrison, I. T. *J. Chem. Soc., Chem. Commun.* **1972**, 231–232. (c) Schill, G.; Beckmann, W.; Schweikert, F. H. *Chem. Ber.* **1986**, *119*, 2647–2655.
- (4) (a) Schill, G. C. *Rotaxanes and Knots*; Academic Press: New York, 1971. (b) Schill, G.; Zürcher, C. *Chem. Ber.* **1977**, *110*, 2046–2066. (c) Schill, G.; Rissler, K.; Fritz, H. *Chem. Ber.* **1986**, *119*, 1374–1399. (d) Ünsal, Ö.; Godt, A. *Chem.—Eur. J.* **1999**, *5*, 1728–1733. (e) Hiratani, K.; Suga, J.; Nagawa, Y.; Houjou, H.; Tokuhisa, H.; Numata, M.; Watanabe, K. *Tetrahedron Lett.* **2002**, *43*, 5747–5750. (f) Godt, A. *Eur. J. Org. Chem.* **2004**, 1639–1654. (g) Kameta, N.; Hiratani, K.; Nagawa, Y. *Chem. Commun.* **2004**, 466–467. (h) Hirose, K.; Nishihara, K.; Harada, N.; Nakamura, Y.; Masuda, D.; Araki, M.; Tobe, Y. *Org. Lett.* **2007**, *9*, 2969–2972.
- (5) (a) Dietrich-Buchecker, C. O.; Sauvage, J.-P.; Kintzinger, J.-P. *Tetrahedron Lett.* **1983**, *24*, 5095–5098. (b) Dietrich-Buchecker, C. O.; Sauvage, J.-P.; Kern, J.-M. *J. Am. Chem. Soc.* **1984**, *106*, 3043–3045. (c) Cesario, M.; Dietrich-Buchecker, C. O.; Guilhem, J.; Pascard, C.; Sauvage, J.-P. *J. Chem. Soc., Chem. Commun.* **1985**, 244–247. (d) Sauvage, J.-P. *Nouv. J. Chim.* **1985**, *9*, 299–310. (e) Dietrich-Buchecker, C. O.; Sauvage, J.-P. *Chem. Rev.* **1987**, *87*, 795–810. (f) Dietrich-Buchecker, C. O.; Colasson, B. X.; Sauvage, J.-P. *Top. Curr. Chem.* **2005**, *249*, 261–283. (g) Duroola, F.; Sauvage, J.-P. *Angew. Chem., Int. Ed.* **2007**, *46*, 3537–3540. (h) Prikhod'ko, A. I.; Duroola, F.; Sauvage, J.-P. *J. Am. Chem. Soc.* **2008**, *130*, 448–449. (i) Prikhod'ko, A. I.; Sauvage, J.-P. *J. Am. Chem. Soc.* **2009**, *131*, 6794–6807. (j) Collin, J.-P.; Duroola, F.; Frey, J.; Heitz, V.; Reviriego, F.; Sauvage, J.-P.; Trolez, Y.; Rissanen, K. *J. Am. Chem. Soc.* **2010**, *132*, 6840–6850. (6) Stoddart, J. F. *Chem. Soc. Rev.* **2009**, *38*, 1521–1529.
- (7) Busch, D. H.; Stephenson, N. A. *Coord. Chem. Rev.* **1990**, *100*, 119–154.
- (8) Olsen, J.-C.; Griffiths, K. E.; Stoddart, J. F. In *From Non-Covalent Assemblies to Molecular Machines*; Sauvage, J.-P., Gaspard, P., Eds.; Wiley-VCH: Weinheim, Germany, 2011; pp 67–139.
- (9) (a) Harada, A.; Li, J.; Kamachi, M. *Nature* **1992**, *356*, 325–327. (b) Armspach, D.; Ashton, P. R.; Moore, C. P.; Spencer, N.; Stoddart, J. F.; Wear, T. J.; Williams, D. J. *Angew. Chem., Int. Ed. Engl.* **1993**, *32*, 854–858. (c) Fujita, M.; Ibukuro, F.; Hagihara, H.; Ogura, K. *Nature* **1994**, *367*, 720–723. (d) Anderson, S.; Anderson, H. L. *Angew. Chem., Int. Ed.* **1996**, *35*, 1956–1959. (e) Craig, M. R.; Hutchings, M. G.; Claridge, T. D. W.; Anderson, H. L. *Angew. Chem., Int. Ed.* **2001**, *40*, 1071–1074. (f) Stanier, C. A.; Alderman, S. J.; Claridge, T. D. W.; Anderson, H. L. *Angew. Chem., Int. Ed.* **2002**, *41*, 1769–1772. (g) Wang, Q.-C.; Qu, D.-H.; Ren, J.; Chen, K.; Tian, H. *Angew. Chem., Int. Ed.* **2004**, *43*, 2661–2665. (h) Murakami, H.; Kawabuchi, A.; Matsumoto, R.; Ido, T.; Nakashima, N. *J. Am. Chem. Soc.* **2005**, *127*, 15891–15899. (i) Cheetham, A. G.; Hutchings, M. G.; Claridge, T. D. W.; Anderson, H. L. *Angew. Chem., Int. Ed.* **2006**, *45*, 1596–1599. (j) Zhao, Y.-L.; Dichtel, W. R.; Trabolsi, A.; Saha, S.; Aprahamian, I.; Stoddart, J. F. *J. Am. Chem. Soc.* **2008**, *130*, 11294–11296. (k) Au-Yeung, H. Y.; Pantoş, G. D.; Sanders, J. K. M. *Proc. Natl. Acad. Sci. U.S.A.* **2009**, *106*, 10466–10470. (l) Au-Yeung, H. Y.; Pantoş, G. D.; Sanders, J. K. M. *Angew. Chem., Int. Ed.* **2010**, *49*, 5331–5334. (m) Fang, L.; Basu, S.; Sue, C.-H.; Fahrenbach, A. C.; Stoddart, J. F. *J. Am. Chem. Soc.* **2011**, *133*, 396–399. (n) Cougnon, F. B. L.; Au-Yeung, H. Y.; Pantoş, G. D.; Sanders, J. K. M. *J. Am. Chem. Soc.* **2011**, *133*, 3198–3207.
- (10) (a) Ashton, P. R.; Goodnow, T. T.; Kaifer, A. E.; Reddington, M. V.; Slawin, A. M. Z.; Spencer, N.; Stoddart, J. F.; Vicent, C.; Williams, D. J. *Angew. Chem., Int. Ed. Engl.* **1989**, *28*, 1396–1399. (b) Anelli, P.-L.; Spencer, N.; Stoddart, J. F. *J. Am. Chem. Soc.* **1991**, *113*, 5131–5133. (c) Philp, D.; Stoddart, J. F. *Angew. Chem., Int. Ed. Engl.* **1996**, *35*, 1155–1196. (d) Hamilton, D. G.; Davies, J. E.; Prodi,

- L.; Sanders, J. K. M. *Chem.—Eur. J.* **1998**, *4*, 608–620. (e) Kaiser, G.; Jarrosson, T.; Otto, S.; Ng, Y.-F.; Bond, A. D.; Sanders, J. K. M. *Angew. Chem., Int. Ed.* **2004**, *43*, 1959–1962. (f) Cao, D.; Amelia, M.; Klivansky, L. M.; Koshkakarayan, G.; Khan, S. I.; Semeraro, M.; Silvi, S.; Venturi, M.; Credi, A.; Liu, Y. *J. Am. Chem. Soc.* **2010**, *132*, 1110–1122.
- (11) (a) Hunter, C. A. *J. Chem. Soc., Chem. Commun.* **1991**, 749–751. (b) Hunter, C. A. *J. Am. Chem. Soc.* **1992**, *114*, 5303–5311. (c) Vögtle, F.; Meier, S.; Hoss, R. *Angew. Chem., Int. Ed. Engl.* **1992**, *31*, 1619–1622. (d) Hoss, R.; Vögtle, F. *Angew. Chem., Int. Ed. Engl.* **1994**, *33*, 375–384. (e) Johnston, A. G.; Leigh, D. A.; Pritchard, R. J.; Deagan, M. D. *Angew. Chem., Int. Ed. Engl.* **1995**, *34*, 1209–1212. (f) Leigh, D. A.; Murphy, A.; Smart, J. P.; Slawin, A. M. Z. *Angew. Chem., Int. Ed.* **1997**, *36*, 728–732. (g) Yamamoto, C.; Okamoto, Y.; Schmidt, T.; Jäger, R.; Vögtle, F. *J. Am. Chem. Soc.* **1997**, *119*, 10547–10548. (h) Schmieder, R.; Hübner, G.; Seel, C.; Vögtle, F. *Angew. Chem., Int. Ed.* **1999**, *38*, 3528–3530. (i) Lukin, O.; Kuboto, T.; Okamoto, Y.; Schelhase, F.; Yoneva, A.; Müller, W. M.; Müllner, U.; Vögtle, F. *Angew. Chem., Int. Ed.* **2003**, *42*, 4542–4545. (j) Schalley, C. A.; Reckien, W.; Peyerimhoff, S.; Baytekin, B.; Vögtle, F. *Chem.—Eur. J.* **2004**, *10*, 4777–4789. (k) Chatterjee, M. N.; Kay, E. R.; Leigh, D. A. *J. Am. Chem. Soc.* **2006**, *128*, 4058–4073. (l) D'Souza, D. M.; Leigh, D. A.; Mottier, L.; Mullen, K. M.; Paolucci, F.; Teat, S. J.; Zhang, S. *J. Am. Chem. Soc.* **2010**, *132*, 9465–9470. (m) Ahmed, R.; Altieri, A.; D'Souza, D. M.; Leigh, D. A.; Mullen, K. M.; Pappmeyer, M.; Slawin, A. M. Z.; Wong, J. K. Y.; Woollins, J. D. *J. Am. Chem. Soc.* **2011**, *133*, 12304–12310.
- (12) (a) Glink, P. T.; Schiavo, C.; Stoddart, J. F. *Chem. Commun.* **1996**, 13, 1483–1490. (b) Fyfe, M. C. T.; Stoddart, J. F. *Acc. Chem. Res.* **1997**, *30*, 393–401. (c) Cantrill, S. J.; Pease, A. R.; Stoddart, J. F. *J. Chem. Soc., Dalton Trans.* **2000**, 21, 3715–3734. (d) Aucagne, V.; Leigh, D. A.; Lock, J. S.; Thomson, A. R. *J. Am. Chem. Soc.* **2006**, *128*, 1784–1785. (e) Badjic, J. D.; Ronconi, C. M.; Stoddart, J. F.; Balzani, V.; Silvi, S.; Credi, A. *J. Am. Chem. Soc.* **2006**, *128*, 1489–1499. (f) Wang, X.; Bao, X.; Mancini-McFarland, M.; Isaacsohn, I.; Drew, A. G.; Smithrud, D. B. *J. Am. Chem. Soc.* **2007**, *129*, 7284–7293. (g) Guidry, E. N.; Li, J.; Stoddart, J. F.; Grubbs, R. H. *J. Am. Chem. Soc.* **2007**, *129*, 8944–8945. (h) Jiang, W.; Winkler, H. D. F.; Schalley, C. A. *J. Am. Chem. Soc.* **2008**, *130*, 13852–13853. (i) Clark, P. G.; Guidry, E. N.; Chan, W. Y.; Steinmetz, W. E.; Grubbs, R. H. *J. Am. Chem. Soc.* **2010**, *132*, 3405–3412.
- (13) (a) Hübner, G. M.; Gläer, J.; Seel, C.; Vögtle, F. *Angew. Chem., Int. Ed.* **1999**, *38*, 383–386. (b) Reuter, C.; Wienand, W.; Hübner, G. M.; Seel, C.; Vögtle, F. *Chem.—Eur. J.* **1999**, *5*, 2692–2697. (c) Schalley, C. A.; Silva, G.; Nising, C. F.; Linnartz, P. *Helv. Chem. Acta* **2002**, *85*, 1578–1596. (d) Mahoney, J. M.; Shukla, R.; Marshall, R. A.; Beatty, A. M.; Zajicek, J.; Smith, B. D. *J. Org. Chem.* **2002**, *67*, 1436–1440. (e) Deetz, M. J.; Shukla, R.; Smith, B. D. *Tetrahedron* **2002**, *58*, 799–805. (f) Wisner, J. A.; Beer, P. D.; Drew, M. G. B.; Sambrook, M. R. *J. Am. Chem. Soc.* **2002**, *124*, 12469–12476. (g) Sambrook, M. R.; Beer, P. D.; Wisner, J. A.; Paul, R. L.; Cowley, A. R. *J. Am. Chem. Soc.* **2004**, *126*, 15364–15365. (h) Curiel, D.; Beer, P. D. *Chem. Commun.* **2005**, 1909–1911.
- (14) (a) Trabolzi, A.; Khashab, N.; Fahrenbach, A. C.; Friedman, D. C.; Colvin, M. T.; Cotí, K. K.; Benítez, D.; Tkatchouk, E.; Olsen, J.-C.; Belowich, M. E.; Carmielli, R.; Khatib, H. A.; Goddard, W. A. III; Wasielewski, M. R.; Stoddart, J. F. *Nat. Chem.* **2010**, *2*, 42–49. (b) Li, H.; Fahrenbach, A. C.; Coskun, A.; Zhu, Z.; Barin, G.; Zhao, Y.-L.; Botros, Y. Y.; Sauvage, J.-P.; Stoddart, J. F. *Angew. Chem., Int. Ed.* **2011**, *50*, 6782–6788.
- (15) Pedersen, C. J. *Aldrichim. Acta* **1971**, *4*, 1–4.
- (16) (a) Pedersen, C. J. *J. Am. Chem. Soc.* **1967**, *89*, 2495–2496. (b) Pedersen, C. J. *J. Am. Chem. Soc.* **1967**, *89*, 7017–7036.
- (17) (a) Lehn, J.-M. *Science* **1985**, *227*, 849–856. (b) Lehn, J.-M. *Angew. Chem., Int. Ed. Engl.* **1988**, *27*, 89–112. (c) Lehn, J.-M. *Angew. Chem., Int. Ed. Engl.* **1990**, *29*, 1304–1319.
- (18) (a) Lehn, J.-M. *Supramolecular Chemistry: Concepts and Perspectives*; Wiley-VCH: Weinheim, Germany, 1995. (b) Stoddart, J. F. *Nat. Chem.* **2009**, *1*, 14–15.
- (19) (a) Cram, D. J.; Cram, J. M. *Science* **1974**, *183*, 803–809. (b) Cram, D. J. *Science* **1983**, *219*, 1177–1183. (c) Cram, D. J. *Angew. Chem., Int. Ed. Engl.* **1988**, *27*, 1009–1020.
- (20) Cram, D. J.; Cram, J. M. *Container Molecules and Their Guests*; Royal Society of Chemistry: Cambridge, U.K., 1994.
- (21) (a) Kyba, E. P.; Siegel, M. G.; Sousa, L. R.; Sogah, G. D. Y.; Cram, D. J. *J. Am. Chem. Soc.* **1973**, *95*, 2691–2692. (b) Kyba, E. P.; Koga, K.; Sousa, L. R.; Siegel, M. G.; Cram, D. J. *J. Am. Chem. Soc.* **1973**, *95*, 2692–2693. (c) Helgeson, R. C.; Koga, K.; Timko, J. M.; Cram, D. J. *J. Am. Chem. Soc.* **1973**, *95*, 3023–3025. (d) Kyba, E. P.; Helgeson, R. C.; Madan, K.; Gokel, G. W.; Tarnowski, T. L.; Moore, S. S.; Cram, D. J. *J. Am. Chem. Soc.* **1977**, *99*, 2564–2571. (e) Timko, J. M.; Helgeson, R. C.; Cram, D. J. *J. Am. Chem. Soc.* **1978**, *100*, 2828–2834. (f) Cram, D. J.; Kaneda, T.; Helgeson, R. C.; Lein, G. M. *J. Am. Chem. Soc.* **1979**, *101*, 6752–6754. (g) Helgeson, R. C.; Mazaleyra, J.-P.; Cram, D. J. *J. Am. Chem. Soc.* **1981**, *103*, 3929–3931. (h) Cram, D. J.; Kaneda, T.; Helgeson, R. C.; Brown, S. B.; Knobler, C. B.; Maverick, E.; Trueblood, K. N. *J. Am. Chem. Soc.* **1984**, *107*, 3645–3657. (i) Paek, K.; Knobler, C. B.; Maverick, E. F.; Cram, D. J. *J. Am. Chem. Soc.* **1989**, *111*, 8662–8671. (j) Judice, J. K.; Cram, D. J. *J. Am. Chem. Soc.* **1991**, *113*, 2790–2791.
- (22) Ashton, P. R.; Campbell, P. J.; Chrystal, E. J. T.; Glink, P. T.; Menzer, S.; Philp, D.; Spencer, N.; Stoddart, J. F.; Tasker, P. A.; Williams, D. J. *Angew. Chem., Int. Ed. Engl.* **1995**, *34*, 1865–1869.
- (23) Kolchinski, A. G.; Busch, D. H.; Alcock, N. W. *J. Chem. Soc. Chem. Commun.* **1995**, 1289–1291.
- (24) (a) Anderson, S.; Anderson, H. L.; Sanders, J. K. M. *Acc. Chem. Res.* **1993**, *26*, 469–475. (b) Cacciapaglia, R.; Manodolini, L. *Chem. Soc. Rev.* **1993**, *22*, 221–231. (c) Hoss, R.; Vögtle, F. *Angew. Chem., Int. Ed.* **1994**, *33*, 375–384. (d) Raymo, F. M.; Stoddart, J. F. *Pure Appl. Chem.* **1996**, *68*, 313–322. (e) Breault, G. A.; Hunter, C. A.; Mayers, P. C. *Tetrahedron* **1999**, *55*, 5265–5293. (f) Hubin, T. J.; Busch, D. H. *Coord. Chem. Rev.* **2000**, *200*, 5–52. (g) Blanco, M.-J.; Chambron, J.-C.; Jiménez, M. C.; Sauvage, J.-P. *Top. Stereochem.* **2002**, *23*, 125–173. (h) Stoddart, J. F.; Tseng, H.-R. *Proc. Natl. Acad. Sci. U.S.A.* **2002**, *99*, 4797–4800. (i) Busch, D. H. *Top. Curr. Chem.* **2005**, *249*, 1–65. (j) Meyer, C. D.; Joiner, C. S.; Stoddart, J. F. *Chem. Soc. Rev.* **2007**, *36*, 1705–1723. (k) Crowley, J. D.; Goldup, S. M.; Lee, A.-L.; Leigh, D. A.; McBurney, R. T. *Chem. Soc. Rev.* **2009**, *38*, 1530–1541.
- (25) (a) Ashton, R. R.; Glink, P. T.; Stoddart, J. F.; Tasker, P. A.; White, A. J. P.; Williams, D. J. *Chem.—Eur. J.* **1996**, *2*, 729–736. (b) Cantrill, S. J.; Fulton, D. A.; Fyfe, M. C. T.; Stoddart, J. F.; White, A. J. P.; Williams, D. J. *Tetrahedron Lett.* **1999**, *40*, 3669–3672. (c) Rowan, S. J.; Cantrill, S. J.; Stoddart, J. F. *Org. Lett.* **1999**, *1*, 129–132. (d) Blanco, M.-J.; Chambron, J.-C.; Heitz, V.; Sauvage, J.-P. *Org. Lett.* **2000**, *2*, 3051–3054. (e) Gunter, M. J.; Bampos, N.; Johnston, K. D.; Sanders, J. K. M. *New J. Chem.* **2001**, *25*, 166–173. (f) Tuncel, D.; Steinke, J. H. G. *Macromolecules* **2004**, *37*, 288–302. (g) Sasabe, H.; Kihara, N.; Furusho, Y.; Mizuno, K.; Ogawa, A.; Takata, T. *Org. Lett.* **2004**, *6*, 3957–3960. (h) Dichtel, W. R.; Miljanić, O. Š.; Spruell, J. M.; Heath, J. R.; Stoddart, J. F. *J. Am. Chem. Soc.* **2006**, *128*, 10388–10390. (i) Wenz, G.; Han, B.-H.; Müller, A. *Chem. Rev.* **2006**, *106*, 782–817. (j) Hsu, C.-C.; Chen, N.-C.; Lai, C.-C.; Liu, Y.-H.; Peng, S.-M.; Chiu, S.-H. *Angew. Chem., Int. Ed.* **2008**, *47*, 7475–7478. (k) Brown, A.; Mullen, K. M.; Ryu, J.; Chmielewski, M. J.; Santos, S. M.; Felix, V.; Thompson, A. L.; Warren, J. E.; Pasco, S. I.; Beer, P. D. *J. Am. Chem. Soc.* **2009**, *131*, 4937–4952. (l) Matsumura, T.; Ishiwari, F.; Koyama, Y.; Takata, T. *Org. Lett.* **2010**, *12*, 3828–3831. (m) Li, H.; Fahrenbach, A. C.; Coskun, A.; Zhu, Z.; Barin, G.; Zhao, Y.-L.; Botros, Y. Y.; Sauvage, J.-P.; Stoddart, J. F. *Angew. Chem., Int. Ed.* **2011**, *50*, 6782–6788. (n) Zheng, H.; Li, Y.; Zhou, C.; Li, Y.; Yang, W.; Zhou, W.; Zuo, Z.; Liu, H. *Chem.—Eur. J.* **2011**, *17*, 2160–2167.
- (26) (a) Ashton, P. R.; Baxter, I.; Fyfe, M. C. T.; Raymo, F. M.; Spencer, N.; Stoddart, J. F.; White, A. J. P.; Williams, D. J. *J. Am. Chem. Soc.* **1998**, *120*, 2297–2307. (b) Hsueh, S.-Y.; Lai, C.-C.; Liu, Y.-H.; Wang, Y.; Peng, S.-M.; Chiu, S.-H. *Org. Lett.* **2007**, *9*, 4523–4526. (c) McConnell, A. J.; Beer, P. D. *Chem.—Eur. J.* **2011**, *17*, 2724–2733.
- (27) Glink, P. T.; Olivia, A. I.; Stoddart, J. F.; White, A. J. P.; Williams, D. J. *Angew. Chem., Int. Ed.* **2001**, *40*, 1870–1875.

- (28) (a) Brady, P. A.; Bonar-Law, R. P.; Rowan, S. J.; Suckling, C. J.; Sanders, J. K. M. *Chem. Commun.* **1996**, 319–320. (b) Brady, P. A.; Sanders, J. K. M. *Chem. Soc. Rev.* **1997**, 26, 327–336. (c) Lehn, J.-M. *Chem.—Eur. J.* **1999**, 5, 2455–2463. (d) Sanders, J. K. M. *Pure Appl. Chem.* **2000**, 72, 2265–2274. (e) Grieg, L. M.; Philp, D. *Chem. Soc. Rev.* **2001**, 30, 287–302. (f) Furlan, R. L. E.; Otto, S.; Sanders, J. K. M. *Proc. Natl. Acad. Sci. U.S.A.* **2002**, 99, 4801–4804. (g) Rowan, S. J.; Cantrill, S. J.; Cousins, G. R. L.; Sanders, J. K. M.; Stoddart, J. F. *Angew. Chem., Int. Ed.* **2002**, 41, 898–952. (h) Corbett, P. T.; Leclaire, J.; Vial, L.; West, K. R.; Wietor, J.-L.; Sanders, J. K. M.; Otto, S. *Chem. Rev.* **2006**, 106, 3652–3711. (i) Lehn, J.-M. *Chem. Soc. Rev.* **2007**, 36, 151–160. (j) Granzhan, A.; Riis-Johannessen, T. *Angew. Chem., Int. Ed.* **2010**, 49, 5515–5518.
- (29) Horn, M.; Ihringer, J.; Glink, P. T.; Stoddart, J. F. *Chem.—Eur. J.* **2003**, 9, 4046–4054.
- (30) (a) Shen, Y. X.; Gibson, H. W. *Macromolecules* **1992**, 25, 2058–2059. (b) Harada, A.; Li, J.; Kamachi, M. *Nature* **1992**, 356, 325–327. (c) Harada, A.; Li, J.; Kamachi, M. *J. Am. Chem. Soc.* **1994**, 116, 3192–3196. (d) Lee, S.-H.; Gibson, H. W. *Macromolecules* **1997**, 30, 5557–5559. (e) Gibson, H. W.; Engen, P. T.; Lee, S.-H. *Polymer* **1999**, 40, 1823–1832. (f) Kihara, N.; Hinoue, K.; Takata, T. *Macromolecules* **2005**, 38, 223–226. (g) Arai, T.; Takata, T. *Chem. Lett.* **2007**, 36, 418–419. (h) Arai, T.; Hayashi, M.; Takagi, N.; Takata, T. *Macromolecules* **2009**, 42, 1881–1887. (i) Nakazono, K.; Takashima, T.; Arai, T.; Koyama, Y.; Takata, T. *Macromolecules* **2010**, 43, 691–696. (j) Kohsaka, Y.; Koyama, Y.; Takata, T. *Angew. Chem., Int. Ed.* **2011**, 50, 10417–10420.
- (31) (a) Sohga, Y.; Fujimori, H.; Shoji, J.; Furusho, Y.; Kihara, N.; Takata, T. *Chem. Lett.* **2001**, 774–775. (b) Oku, T.; Furusho, Y.; Takata, T. *J. Polym. Sci. Part A* **2003**, 41, 119–123. (c) Lee, Y.-G.; Koyama, Y.; Yonekawa, M.; Takata, T. *Macromolecules* **2010**, 43, 4070–4080.
- (32) (a) Delaviz, Y.; Gibson, H. W. *Macromolecules* **1992**, 25, 4859–4862. (b) Gong, C.; Gibson, H. W. *J. Am. Chem. Soc.* **1997**, 119, 5862–5866. (c) Gong, C.; Gibson, H. W. *J. Am. Chem. Soc.* **1997**, 119, 8585–8591.
- (33) (a) Amabilino, D. B.; Stoddart, J. F. *Chem. Rev.* **1995**, 95, 2725–2828. (b) Raymo, F. M.; Stoddart, J. F. *Chem. Rev.* **1999**, 99, 1643–1663. (c) Dietrich-Buchecker, C.; Sauvage, J.-P., Eds.; *Molecular Catenanes, Rotaxanes, and Knots. A Journey Through the World of Molecular Topology*; Wiley-VCH: Weinheim, Germany, 1999. (d) Huang, F.; Gibson, H. W. *Prog. Polym. Sci.* **2005**, 30, 982–1018. (e) Harada, A. *J. Polym. Sci., Polym. Chem.* **2006**, 44, 5113–5119. (f) Takata, T. *Polym. J.* **2006**, 38, 1–20. (g) Wenz, G.; Han, B.-H.; Müller, A. *Chem. Rev.* **2006**, 106, 782–817. (h) Harada, A.; Hashidzume, A.; Yamaguchi, H.; Takashima, Y. *Chem. Rev.* **2009**, 109, 5974–6023. (i) Fang, L.; Olson, M. A.; Benítez, D.; Tkatchouk, E.; Goddard, W. A. III; Stoddart, J. F. *Chem. Soc. Rev.* **2010**, 39, 17–29.
- (34) Wu, J.; Leung, K. C.-F.; Stoddart, J. F. *Proc. Natl. Acad. Sci. U.S.A.* **2007**, 104, 17266–17271.
- (35) Belowich, M. E.; Valente, C.; Stoddart, J. F. *Angew. Chem., Int. Ed.* **2010**, 49, 7208–7212.
- (36) Momčilović, N.; Clark, P. G.; Boydston, A. J.; Grubbs, R. H. *J. Am. Chem. Soc.* **2011**, 133, 19087–19089.
- (37) The degree of polymerization (DP) can be calculated by the Carothers equation which states that $DP = 1/(1-p)$, where p is the conversion to polymer defined by $p = (N_0 - N)/N_0$, where N_0 is the number of molecules present initially and N is the number of unreacted molecules at time t . Stevens, M. P. *Polymer Chemistry: An Introduction*; Oxford University Press: New York, 1999.
- (38) (a) Zhao, A.; Moore, J. S. *J. Am. Chem. Soc.* **2002**, 124, 9996–9997. (b) Zhao, D.; Moore, J. S. *J. Am. Chem. Soc.* **2003**, 125, 16294–16299. (c) Janssen, P. G. A.; Jabbari-Farouji, S.; Surin, M.; Vila, X.; Gielen, J. C.; de Greef, T. F. A.; Vos, M. R. J.; Bomans, P. H. H.; Sommerdijk, N. A. J. M.; Christianen, P. C. M.; Leclère, P.; Lazzaroni, R.; van der Schoot, P.; Meijer, E. W.; Schenning, A. P. H. J. *J. Am. Chem. Soc.* **2009**, 131, 1222–1231. (d) Olson, M. A.; Coskun, A.; Fang, L.; Basuray, A. N.; Stoddart, J. F. *Angew. Chem., Int. Ed.* **2010**, 49, 3151–3156.
- (39) (a) Yamauchi, Y.; Yoshizawa, M.; Fujita, M. *J. Am. Chem. Soc.* **2008**, 130, 5832–5833. (b) Yamauchi, Y.; Yoshizawa, M.; Akita, M.; Fujita, M. *J. Am. Chem. Soc.* **2010**, 132, 960–966.
- (40) Thiel, J.; Yang, D.; Rosnes, M. H.; Liu, X.; Yvon, C.; Kelly, S. E.; Song, Y. F.; Long, D. L.; Cronin, L. *Angew. Chem., Int. Ed.* **2011**, 50, 8871–8875.
- (41) Investigations by IMS-MS on the higher-order oligorotaxanes were prevented by not being able to obtain stable ion-sprays.
- (42) Data were collected at 100 K using a Bruker d8-APEX II CCD diffractometer (Cu K α radiation, $\lambda = 1.54178$ Å). Intensity data were collected using ω and φ scans spinning at least a hemisphere of reciprocal space for all structures (data were integrated using SAINT). Absorption effects were collected on the basis of multiple equivalent reflections (SADABS). Structures were solved by direct methods (SHELXS) and refined by full-matrix least-squares against F^2 (SHELXL). Hydrogen atoms were assigned riding isotropic displacement parameters and constrained to idealized geometries. Crystallographic data (excluding structure factors) for the structures reported in this article have been deposited with the Cambridge Crystallographic Data Center as supplementary publication no. CCDC-826138 (2R·2PF₆) and CCDC-826139 (3R·3PF₆). Copies of the data can be obtained free of charge on application to CCDC, 12 Union Road, Cambridge CB2 1EZ (fax: int. code (44) 1223 336–033; E-mail: deposit@ccdc.cam.ac.uk).
- (43) Crystal data for 2R·2PF₆. C₇₅H₉₀F₁₂N₈O₁₄P₂·CH₂Cl₂·(C₃H₇)₂O. $M = 1804.59$, space group $P1$, triclinic, $a = 13.4795(5)$, $b = 14.5068(4)$, $c = 24.8176(7)$ Å, $\alpha = 85.849(2)^\circ$, $\beta = 88.703(2)^\circ$, $\gamma = 62.846(2)^\circ$, $V = 4306.4(2)$ Å³, $Z = 2$, $\rho_{\text{calc}} = 1.392$ g cm⁻³, $\mu = 1.839$ mm⁻¹, 13912 reflections collected, 13912 observed independent reflections ($R_{\text{int}} = 0.0000$) gave $R = 0.0601$ for $I > 2\sigma(I)$ and $wR_2 = 0.1616$.
- (44) Crystal data for 3R·3PF₆. C₁₀₃H₁₂₇F₁₈N₁₂O₁₉P₃. $M = 2296.10$, space group $P2_1/n$, monoclinic, $a = 16.3196(4)$, $b = 31.1755(7)$, $c = 22.7396(5)$ Å, $\alpha = 90.000(2)^\circ$, $\beta = 95.673(2)^\circ$, $\gamma = 90.000(2)^\circ$, $V = 11512.6(5)$ Å³, $Z = 4$, $\rho_{\text{calc}} = 1.325$ g·cm⁻³, $\mu = 1.320$ mm⁻¹, 78337 reflections collected, 18089 observed independent reflections ($R_{\text{int}} = 0.0765$) gave $R = 0.0840$ for $I > 2\sigma(I)$ and $wR_2 = 0.2296$.
- (45) Raymo, F. M.; Houk, K. N.; Stoddart, J. F. *J. Am. Chem. Soc.* **1998**, 120, 9318–9322.
- (46) Simulations were performed using the molecular dynamics package as implemented in Schrödinger's MacroModel 9.0 software suite, www.schrodinger.com.
- (47) Luening, U.; Baumstark, R.; Peters, K.; von Schnering, H.-G. *Liebigs Ann.* **1990**, 129–143.
- (48) Sieger, H.; Vögtle, F. *Liebigs Ann.* **1980**, 425–440.